International Institute for
Applied Systems Analysis
IIASA www.iiasa.ac.at

CHARM: A Hydrologic Model for Land Use and Climate Change Studies in China

Wiberg, D. and Strzepek, K.M.

IIASA Interim Report
December 2000

International Institute for
Applied Systems Analysis
Schlossplatz 1
A-2361 Laxenburg, Austria

Tel: +43 2236 807 342
Fax: +43 2236 71313
E-mail: publications@iiasa.ac.at
Web: www.iiasa.ac.at

Interim Report **IR-00-072**

CHARM: A Hydrologic Model for Land Use and Climate Change Studies in China

David A. Wiberg (wiberg@iiasa.ac.at)

Kenneth M. Strzepek (strzepek@spot.colorado.edu)

Approved by

Günther Fischer (fisher@iiasa.ac.at)
Leader, Land Use Change Project

December, 2000

Contents

Abstract

China is a country, which is rapidly changing and developing. The population is enormous and still increasing and the economy is growing at a rate that is one of the world's fastest. These factors are placing substantial stress on China's natural resources. Already, the best agricultural land is used and cities are expanding on top of some of this fertile land. Cities are growing so fast that improving and increasing electric and water infrastructure cannot keep up with demand. Much of Northern China is already in a situation of severe water stress.

In order to understand how the resource stress will affect China's development, knowledge of the currently available resource in any area is necessary. Furthermore, possible changes in the resource availability in the future must be understood. These changes could be natural or anthropogenic ranging from climate change to changing land from pasture to irrigated farmland. If good data is available, the current resource availability is already known for all areas and a model can be used to investigate the impacts of any changes to the system. However, if good data is not available, a model must be used to gain both the current state and the impacts of changes. The latter is the method employed here to assess China's water availability.

In this paper, a hydrologic model is developed to assess China's water availability. CHARM, for Climate and Human Activities sensitive Runoff Model, is developed to provide the runoff produced from rainfall throughout China on a 5 km x 5 km grid-cell resolution. The model is calibrated to average annual watershed runoff values. CHARM can then not only supply currently available surface water runoff for entire regions, but can supply runoff and runoff variability inter-annually and intra-annually for any area desired. Furthermore, it can be used to assess the impacts of land use and climate change on water resources. Here, the methodology of CHARM is developed and validated on two watersheds in the yellow river basin in China. It is then used to assess the current water resource supply in China. Finally, the strengths and weaknesses in the model and the modeling approach are discussed to assist the modeler in interpreting the results.

CHARM: A Hydrologic Model for Land Use and Climate Change Studies in China

David A. Wiberg, Kenneth M. Strzepek

1. Introduction

With China's recent rapid economic and population growth, water supply for industry, agriculture, and the growing population is becoming a critical issue. It is estimated that the total renewable freshwater resources of China are 2,700 km^3. Water withdrawals for all uses in 1995 are estimated to be 526 km^3. This results in a Use to Availability Ratio of 0.20. (Shiklamonav, 1999). A national Use to Availability Ratio of 0.2 is considered an indicator that the country is at the low-end of the moderately water stressed categorization. It does indicate that regions of the country are facing water stress.

Which regions are currently facing water stress and which regions in the future under scenarios of economic growth, land-use change and climate change will face water stress cannot be determined using historical observed stream flow. Stream flow is a function of climate and the land surface. With a changing climate due to local and global greenhouse gas and pollution emissions, a detailed spatial model of runoff driven by climate variables and accounting for land use change is needed to estimate future runoff, regionally and nationally. The runoff model should be coupled with a reservoir storage model to determine firm water supply. Then, the water supply should be linked with a water demand model to examine future water stress. These three modeling efforts are under development at the Land Use Change Project at IIASA.

In this report, the hydrologic model, the **C**limate and **H**uman **A**ctivities – sensitive **R**unoff **M**odel or **CHARM**, is developed as one part in assessing the water availability in China and its variability. Section 1 discusses in detail the water balance components that are the physical basis for the model. Section 2 describes the larger structure of the model and how these components have been put together to model entire basins and regions. The third section will apply the model at the basin and national scale. On the basin scale, the model will be tested on two hydro-climatologically different sub-basins of the Yellow River in China. Analyses of the impacts of climate and land use changes on the available water in these basins will be performed. The model will then be applied to the nine major water resource regions of China to estimate the natural available water supply. Finally, conclusions will be discussed in the fourth section.

2. Model component description

2.1. Water balance

Because of the LUC project's interest in how changes in land use as well as climate are affecting China's development, any hydrologic model developed to assess the water resources in China must be sensitive to land cover, land use and management practices. This problem is not a new one and the fact that runoff can vary considerably in time and volume with different land cover, land use, and management practices is well known. As early as 1972, the Soil Conservation Service in the United States had published a method for estimating direct runoff from storm rainfall that addressed this problem for direct runoff. (SCS, 1985) The method was the result of decades of research and has been evolving ever since. In 1986, the Soil Conservation Service developed the TR-55 model, using this 'curve-number' method, with the specific goal of assessing the effects of urban development on runoff (SCS, 1986). The 'curve-number' method has also been used as the direct runoff component in the HELP (Hydrologic Evaluation of Landfill Performance) model used by the US Environmental Protection Agency (EPA, 1994), the SWAT (Soil Water Assessment Tool) model (USDA, 1994) and many others. Because of its wide acceptance and ability to handle different soil types, land use, and management practices, the 'curve number' method is also used as the direct runoff component of CHARM. Once direct runoff is abstracted, the remaining water enters the soil moisture zone where a relatively simple water balance is done, abstracting water for evapotranspiration and sub-surface runoff. The overall structure of the water balance used in the hydrologic model is depicted below in Figure 1:

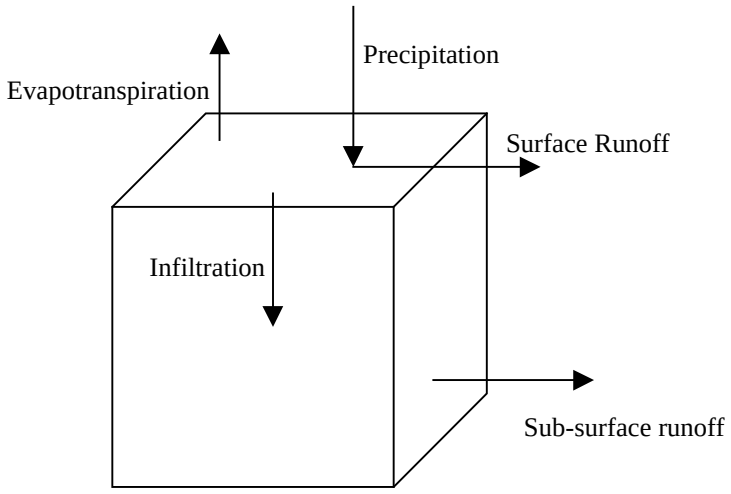

Figure 1: Structure of water balance used in CHARM

As shown in Figure 1, the water balance consists of five components: precipitation, surface runoff, infiltration, evapotranspiration, and sub-surface runoff. A water balance equation describing the above figure can be written as:

$$S_{\max}\frac{dz}{dt} = P(t) - SR(z,t) - E(Et_0, z, t) - SSR(z,t) \qquad \textbf{Equation 1}$$

where

S_{max} ≡ maximum soil storage capacity

z ≡ relative soil storage ($0 \le z \le 1$)

P ≡ precipitation

SR ≡ direct Runoff

E ≡ evapotranspiration

SSR ≡ sub-surface runoff

Each of the components of this water balance is discussed in the following sections.

2.2. Precipitation

Precipitation is given as input to the model and is discussed later with the other model inputs.

2.3. Surface Runoff

As discussed above, direct runoff is calculated by CHARM according to the curve number method. The basic premise of the SCS method is that the ratio of direct runoff to total precipitation after an initial abstraction is the same as the ratio of water retained in the soil to the maximum soil retention:

$$\frac{DR}{P - I_a} = \frac{R}{R_{\max}} \qquad \textbf{Equation 2}$$

where

I_a ≡ the initial water abstraction before any runoff will occur (mm)

R ≡ water retained in the watershed (mm)

R_{max} ≡ maximum retention in the watershed (mm)

DR ≡ direct runoff (mm)

By the continuity principle:

$$R = (P - I_a) - DR \qquad \textbf{Equation 3}$$

Substituting equation 3 into equation 2 yields:

$$\frac{P - I_a - DR}{R_{\max}} = \frac{DR}{P - I_a} \qquad \textbf{Equation 4}$$

An empirical relationship was developed for the initial abstraction and is:

$$I_a = 0.2 R_{\max} \qquad \textbf{Equation 5}$$

Substituting equation 5 into Equation 4 and solving for direct runoff now gives:

$$DR = \frac{(P - 0.2R_{\max})^2}{(P + .8R_{\max})}$$ **Equation 6**

Now, plotting direct runoff over precipitation for many watersheds, the SCS found a family of curves and developed a dimensionless constant, the curve number (CN), to describe these curves. The curve number varies from 0 to 100 and depends on land use, management practices, and soil type. The curve number can be used to calculate the maximum retention (in mm) by the following formula:

$$R_{\max} = 254(\frac{100}{CN} - 1)$$ **Equation 7**

Tables of curve numbers match land use and management practices and soil types to obtain a curve number for those conditions. A small, sample curve number table is shown in Table 1 below:

Land Use	**Hydrologic Soil Group**			
	A	B	C	D
Cultivated Land: without conservation treatment	72	81	88	91
Cultivated Land: with conservation treatment	62	71	78	81
Pasture or range land: poor condition	68	79	86	89
Pasture or range land: good condition	39	61	74	80
Wood or forest land: thin stand, poor cover, no mulch	30	58	71	78
Wood or forest land: good cover	25	55	70	77
Commercial and business areas (85% impervious)	89	92	94	95
Industrial districts (72% impervious)	81	88	91	93
Residential: 1 acre lot size (20% impervious)	51	68	79	84
Residential: 1/2 acre lot size (25% impervious)	54	70	80	85
Residential: 1/8 acre lot size (65% impervious)	77	85	90	92
Paved parking lots, roofs, driveways, etc.	98	98	98	98

Table 1: Sample SCS curve number table

The LUC soil types and land use categories were matched with the SCS land use tables to obtain curve numbers for China. Since slope data is available, a slope adjustment is also made by CHARM to the curve number by the following formula (USDA, 1994, p. 13):

$$CN_{2s} = \frac{1}{3}(CN_2 - CN_1)[1 - 2\exp(-13.86SL)] + CN_2$$ **Equation 8**

where

CN_{2s} ≡ curve number for antecedent moisture condition 2 corrected for slope

CN_{2} ≡ curve number for antecedent moisture condition 2

CN_{1} ≡ curve number for antecedent moisture condition 1

SL ≡ slope (m/m)

The curve number for antecedent moisture condition 1 can be found from the following equation:

$$CN_1 = CN_2 - \frac{20(100 - CN_2)}{100 - CN_2 + \exp[2.533 - 0.0636(100 - CN_2)]}$$ **Equation 9**

The curve numbers, then, allow for the calculation of surface runoff according to equation 6. The remaining rainwater that does not run off directly infiltrates into the soil, where it is influenced by evapotranspiration and sub-surface runoff as described in the following sections.

2.4. Evapotranspiration

To calculate evapotranspiration, CHARM applies a method recommended by FAO (FAO, 1998) and similar to the method used in the Agro-Ecological Zoning Methodology (Fischer *et al*., 2000). Because the estimation of evapotranspiration itself requires a large number of calculations and is discussed in these other sources, the equations are not included here. However, the development of the equations used for evapotranspiration and their implementation in CHARM is discussed completely in Appendix I.

2.5. Sub-Surface Runoff

The final component of the water balance in CHARM is sub-surface runoff (SSR), which accounts for any water that runs off beneath the soil surface by percolating down through the soil. This process is also accomplished quite simply in CHARM by use of a calibration coefficient (α) multiplied by a function of the relative storage (z). (Kaczmarek, 1991; David Yates, 1996; Perrin Bowling, 1997):

$$SSR = \alpha z^2 \qquad \textbf{Equation 10}$$

Referring back to Figure 1, we now see that all the components of the water balance are calculated and Equation 1 is complete. With the methods of the individual components established, we can now go on to look at the larger picture of how the model functions.

3. Model Structure

The last section described the specific details of individual components in the water balance performed by CHARM. This section describes how these components are assembled to model a region or river basin as a whole. The overall structure of the model is depicted in Figure 2:

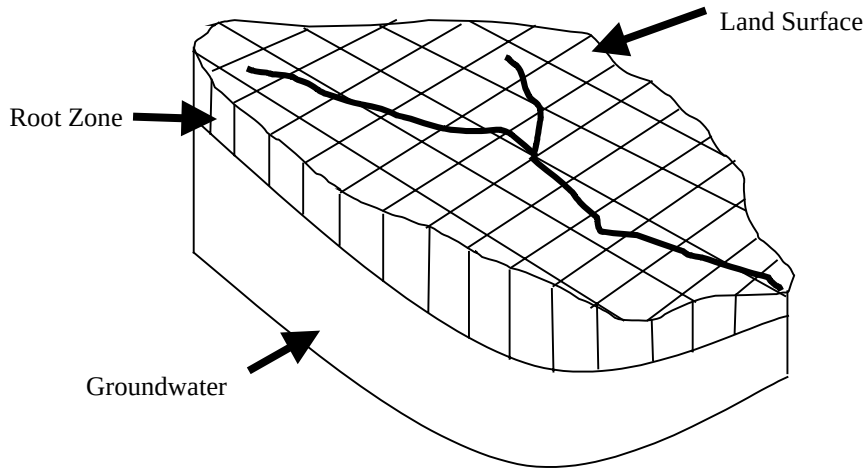

Figure 2: Structure of CHARM.

The figure shows a river basin split into grid cells on the surface with a single groundwater cell beneath. This is actually the most detailed modeling option available in CHARM. Here, surface runoff, evapotranspiration, and sub-surface runoff are modeled in each individual cell. However, a single α parameter is calibrated for the entire basin, since data is not available for runoff in each cell.

Although the figure shows the river basin split into grid-cells, many other configurations are also possible in CHARM. The entire basin can be modeled as a unit with the average curve number and a single station daily rain input. It can also be modeled by creating 'virtual' basins where grid cells with similar land use, management practices, and soil types within the basin are lumped together to form a modeling unit. Both of these methods produce more rapid calculations, but at the expense of information at individual pixels. In many cases, however, there is little variation among the different modeling methods (Bowling and Strzepek, 1998). It is important to note that the primary reason to model at the grid-cell level is that output from this approach may be aggregated differently later, as is done in the modeling of China.

3.1. Inputs to CHARM

To understand how CHARM functions, knowledge of the inputs and how they are used to produce the output, runoff, is necessary. A table of the inputs and a brief description is listed below. A more detailed description of how some of the inputs are used is provided in the following sections.

Input	Used to calculate	Description
Precipitation	Runoff	Rainfall can be input as average monthly values from a spatial grid or it can be entered as daily rainfall from individual stations.
Curve number table	Surface runoff	The curve number table must include curve numbers for all the combinations of land use and soil types in the area to be modeled.
Slope	Surface runoff	Slope (m/m) is input at the same scale as the scale of the simulation: grid-cell, virtual basin, or basin.
Average temperature	Evapotranspiration	Average temperature is input by grid-cell. Monthly averages (in °C) are currently used, since time series data was not available at the time of development.
Temperature range	Evapotranspiration	The monthly average temperature range is used to produce values of the maximum and minimum temperatures. Input is grid-cell, the same as mean temperature.
Sunshine hours per day	Evapotranspiration	Sunshine hours are also input at the grid-cell scale as average monthly values.
Latitude	Evapotranspiration	Latitude (in decimal degrees) is used in the calculations as well as to keep track of the location of the grid-cells.
Longitude	Evapotranspiration	Longitude (in decimal degrees) is used in the same style as latitude.
Altitude	Evapotranspiration	Altitude (m) is also used like latitude.
Land use	Surface runoff	Land use is input on the grid-cell scale and is used in the SCS method.
Soil texture	Surface runoff	Same as land use
Available water content	Water balance and sub-surface runoff	The available water content (mm/m) of the soil is the maximum soil storage minus the wilting point storage per meter of soil.
Soil depth	Water balance and sub-surface runoff	Soil Depth (cm), when multiplied by the available water content gives the total amount of water that can be used in the soil. This is the figure used for the maximum soil storage.
α (optional)	Sub-surface runoff	α can be input to the model or can be calibrated within the model.
α bounds (optional)	Sub-surface runoff/ calibration	The α bounds are used to set bounds on, or bracket, α in the bisection method that is used when calibrating.
α tolerance (optional)	Sub-surface runoff/ calibration	The bisection method calibrates to the maximum error specified by the α tolerance.
Maximum iterations(opt)	Sub-surface runoff/ calibration	Once the calibration loop has gone through the maximum iterations, it will end and the best value of α will be used.
Station/year	Runoff	A region ID and the year to simulate must be input and be consistent throughout files.
Precipitation station (opt)	Runoff	If not using grid-cell rainfall data or the nearest rain gauge, the user can input a single rain gauge to use for the calculations.
Actual runoff (opt)	Calibration	In order to calibrate the model, actual annual runoff must be given corresponding to a year of precipitation data.
Starting soil moisture (opt)	Runoff	In the first time period, the soil moisture is zero, unless set by the modeler here.
Crop coefficient	Evapotranspiration	The user may input an annual average crop coefficient to use in calculating evapotranspiration.
Multipliers	Runoff and climate change	Many components of the model may be increased or decreased for sensitivity studies, better calibration, or climate change studies using multipliers. Multipliers are available for the curve number, maximum soil storage, average temperature, maximum and minimum temperature, and precipitation.
Modeling options	Runoff	Several modeling options can be input to control the model and its components.

Table 2: Inputs to CHARM

3.1.2. Precipitation

Precipitation is input to CHARM as either monthly values at grid-cell scale or as daily values from individual stations. If monthly grid-cell values are used and a series of daily values are available at some scale, daily precipitation is calculated by finding the ratio of the daily value to the monthly average value and using this ratio to find the daily precipitation values for other years. Otherwise spline interpolation (Press *et al*., 1992) is used to calculate daily values from monthly values.

Actual daily values, however, are highly preferred. To illustrate why, consider a storm in a single day of the month that dumps 400 mm of rain, which is the only rain that occurs that month. If the soil can only store 100 mm of water, at least 300 mm of this rainfall must run off. The runoff will even be higher if the storm intensity is greater and the water cannot infiltrate into the soil fast enough and be stored in the soil. On the other hand, if only 400 mm of rain fell over the entire month and were spread throughout the month, then only about 13 mm fell per day. Due to evapotranspiration and percolation, the soil layer may never become saturated and surface runoff might not occur at all. For this reason, daily time-series precipitation data produces more accurate results that also are more sensitive to land use and management practices.

In the current implementation of CHARM, daily precipitation at individual stations is used and the Theissen method is applied to generate daily time-series values for precipitation at the grid-cell level. The Theissen method assumes that the precipitation at any point is the same as that at the nearest gauge (Chow, 1988). It is also possible in CHARM to select a particular station to use when modeling a basin. However, this is only included for flexibility which can be useful when a few years of precipitation data at another station are not available.

3.1.3. Other climatic and physical data

The application of other climatic and physical data is relatively straightforward as described in Table 2. Again, daily time-series of all the climatic data would be ideal. However, temperature and sunshine hours do not vary on a day-to-day basis as widely as precipitation does and are not as influential in calculating monthly runoff as precipitation. Therefore, average monthly temperature and sunshine values are converted to pseudo-daily values using a spline interpolation.

3.2. Calibration

Several of the input coefficients in Table 2 are used only for assisting the process of calibrating the model. These parameters are optional, since the model may be used to calibrate the coefficient α (equation 10) or may be applied with a given α. When the model is used to calibrate α, it does so using a bisection method (Press *et al*, 1992, p. 353). This method of root finding requires that the root be bracketed so that an upper and lower bound for α must be input. Also, a tolerance must be input to specify the accuracy of the iterative numerical procedure desired by the modeler. Finally, the maximum number of iterations input stops the calibration loop in case a root is not found. In this case the best value of α obtained during any of the iterations done is used.

4. Case Studies

To test and validate CHARM, runoff data was obtained from stations on tributaries of the Yellow River. The location of each station is on the tributary, but near the confluence of the tributary with the Yellow River. Basins were chosen that were between 20,000 and 50,000 square kilometers so that the water could easily travel from one end of the watershed to another within a month and routing techniques would not be necessary. These test basins provide good examples of how the model can be used and the results produced. Two of these basins, the Tao He and the Yilou He are described here in detail along with the results of modeling them with CHARM. The locations of the basins within China are shown below in Figure 3:

Figure 3: Map of China showing the provinces, major rivers, and case study basins.

4.1. Tao He

The Tao He flows through the southwestern part of Gansu province where it borders with Qinghai province (See Figure 3). Starting at an elevation of 4000 meters at latitude 34.4 and longitude 101.6, the watershed drops 2000 m over a distance of 470 km. It ends in the upper reach of the Yellow River (the Huang He) at Lanzhou, the capital of Gansu Province, at an elevation of 2000 m, draining an area of about 25000 square kilometers. The watershed consists primarily of grassland but also includes some bare land, bush, timber forest and irrigated and non-irrigated farmland. The region is cold and mountainous and receives an average annual rainfall of 600 mm.

4.1.1. Calibration

In order to calibrate and test CHARM on the Tao He, rainfall and runoff data must be available for the same time period. Daily rainfall data is available from 1951 to 1982 at certain rain gauges in and around the watershed, but only a few years of runoff data is available, 1951, 1980-85, 1987, and 1988. The runoff data is supplied as monthly average stream flows from a stream gauge at Minhe near the confluence of the Tao He with the Yellow River. The raw data are unadjusted for reservoir operations, i.e. not representing the natural, unmanaged flow. Because the data is unadjusted, the best time period for testing the rainfall-runoff relationship is before dams were built in the area. Although a few small dams may have existed, almost all large dams in China were constructed after 1950 (ICOLD, 1984). Therefore, 1951 is the most appropriate year to calibrate the model with available data.

CHARM was set up to calibrate to the 1951 rainfall and runoff data by simulating on a 5 km x 5 km grid. An initial soil moisture of 55 mm was used based on average December conditions. The objective of the calibration was to match the runoff volume for the entire year as a measure of the available resource in the region. The annual flow was obtained by multiplying the average flow rate in each month by the number of seconds in the month and then summing these values for each month in the year. The model is calibrated to this yearly value with a tolerance of 5 percent. Figure 4 shows the model results:

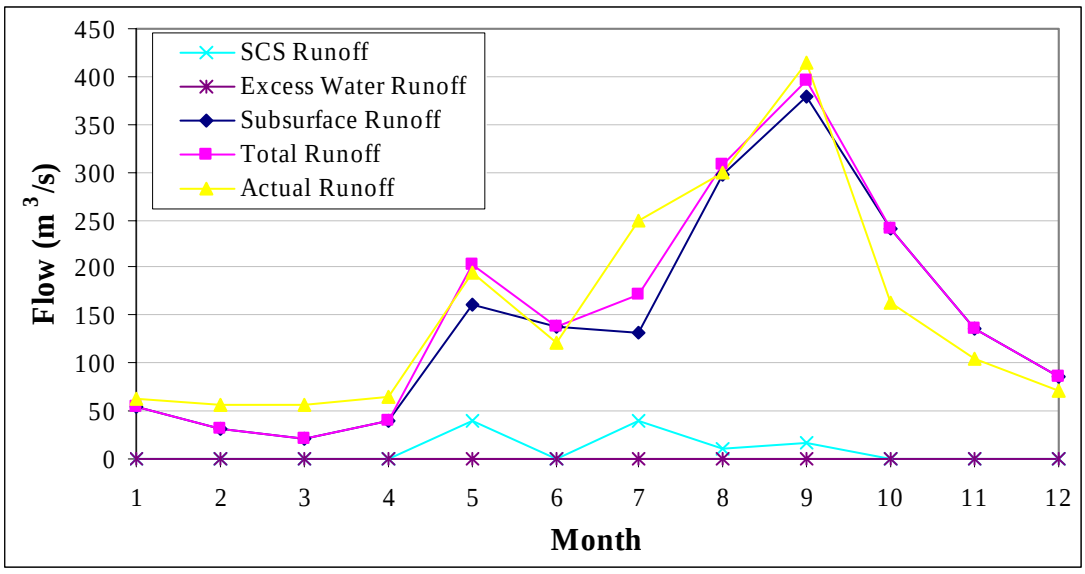

Figure 4: Comparison of actual with total simulated 1951 runoff and its components on the Tao He.

For the Tao He, the coefficient for sub-surface runoff, α, calibrated to 3.125, producing a difference between the actual and simulated year runoff of 1%. Figure 4 shows that although the model was calibrated for yearly runoff, simulated monthly runoff also correlates well with the actual monthly runoff, showing that the dynamics of the system are well modeled. Simulating another year for the same basin produces similar results, as shown by Figure 5:

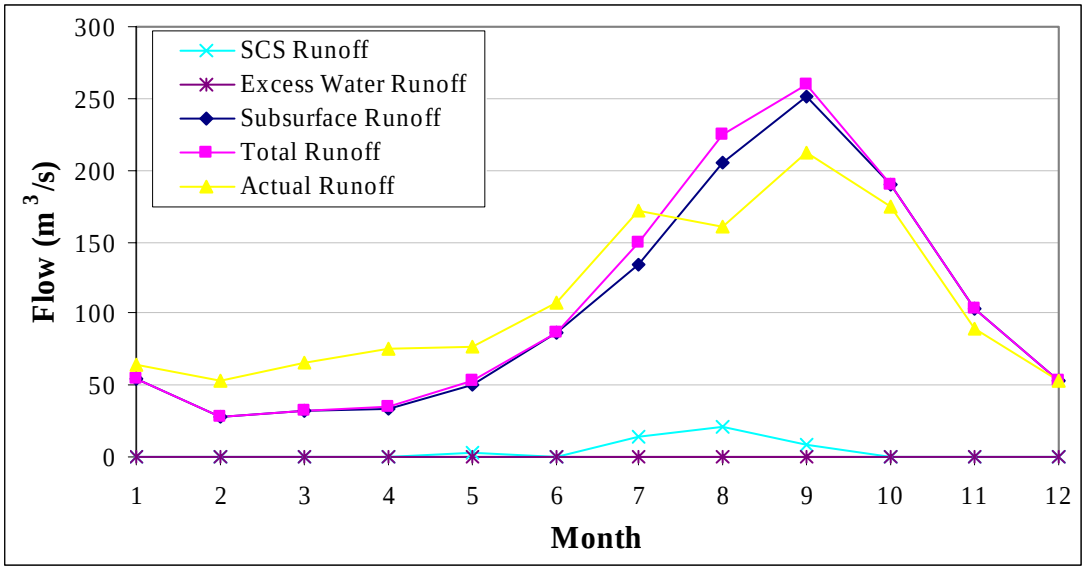

Figure 5: Comparison of actual runoff with total simulated 1980 runoff and its components on the Tao He.

When the model is calibrated based on 1980 data, α again calibrates to 3.125, this time with an annual runoff error of 4%. If the calibration tolerance were set finer than 5%, α would have been slightly different between the two years. However, the fact that α remains very close between the two years indicates that the model is effective and verifies one of the major assumptions in the model methodology, that α is a single sub-surface runoff parameter that describes sub-surface runoff for the basin. Although the simulated monthly runoff in this case does not correlate to actual monthly runoff as well as in 1951, the features of the simulated and actual curves remain similar. An unknown factor that may influence the actual runoff curve and account for the difference is the number of small dams built in the river between 1951 and 1980. At Lanzhou where the Tao He flows into the Yellow River, for example, the Liujiaxia Dam was completed in 1962. Many other dams were built within this time frame, but no data were available for dams on the Tao He.

4.1.2. Sensitivity of the Tao He to Land-Use Change

With CHARM calibrated for the Tao He, we tested the sensitivity of runoff to land-use/cover change in the watershed. This was achieved by quantifying the relationship between monthly runoff in the Tao He basin and a broad range of SCS curve numbers (see Table 1 for the relationship of curve numbers and land uses). The effects of land use change on the Tao He can be seen in Figure 6 and Figure 7.

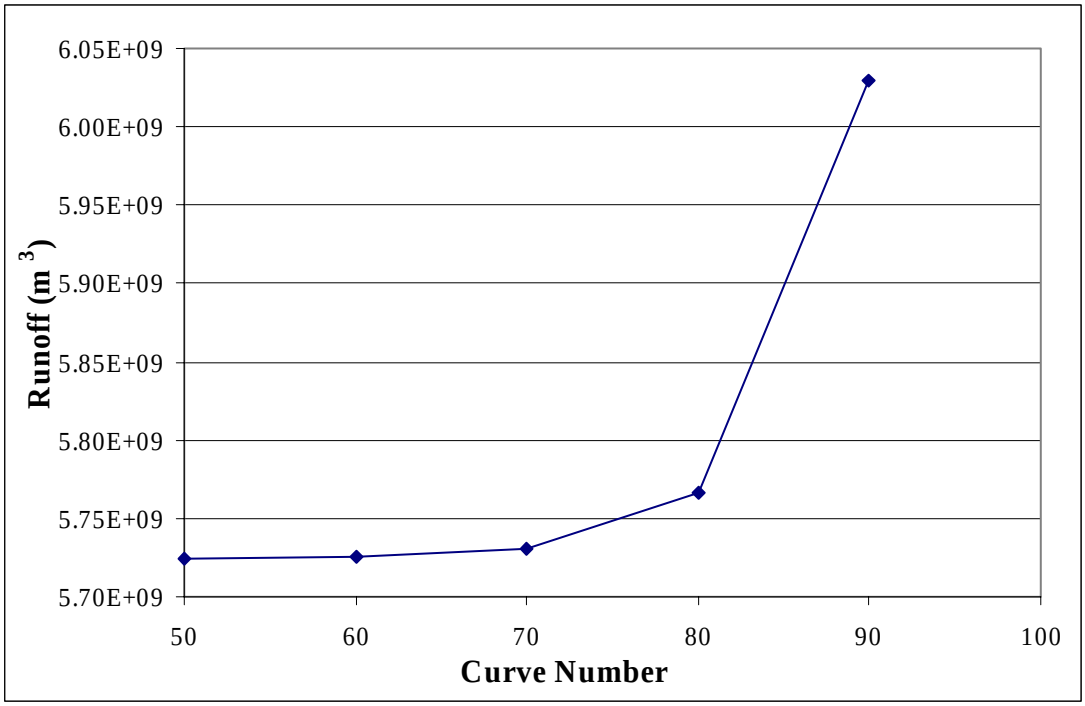

Figure 6: Sensitivity of annual runoff in the Tao He to changes in the curve number

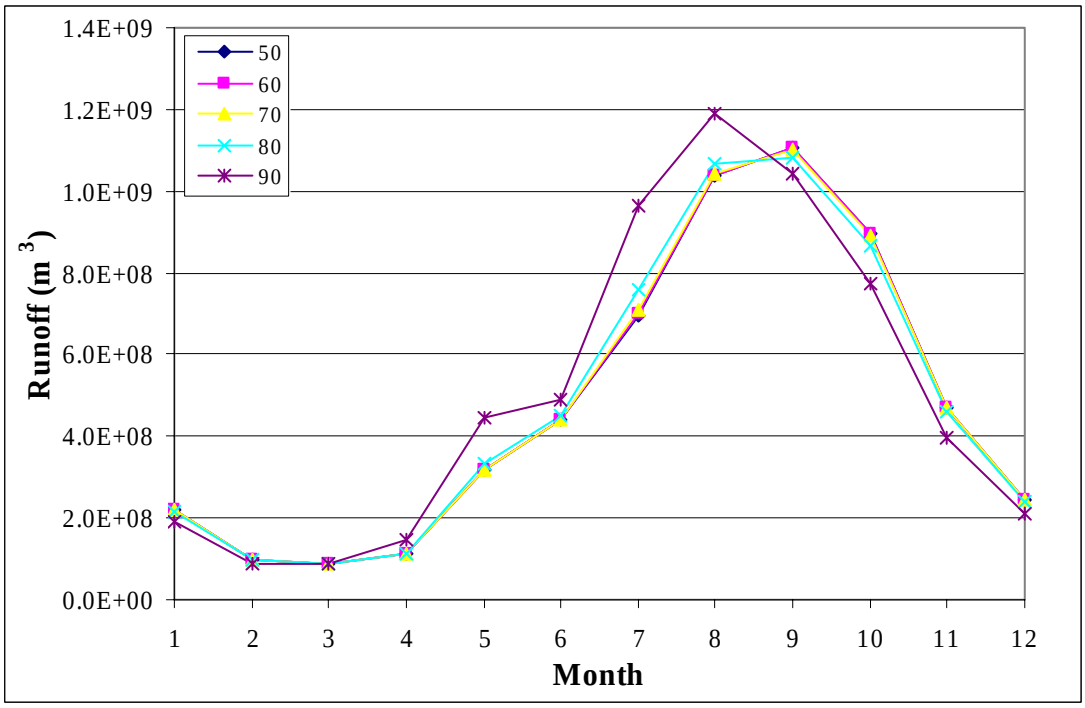

Figure 7: Sensitivity of monthly runoff in the Tao He to changes in the curve number.

The figures show that land use change does not have a large impact on annual flows for the Tao He, with only a 5% difference between a curve number of 50 and 90. This result is not unexpected, however, since the time period of one year is so long. Land use changes produce a greater effect on the timing and variability of flows throughout the year than on annual runoff. Figure 7 also shows that under increasingly impermeable conditions, i.e. increasing SCS curve number, the runoff shifts earlier in the year. This is also expected, as runoff flows more quickly from impermeable land.

4.1.3. Sensitivity of the Tao He to Climate Change

In order to test the sensitivity of the Tao He watershed to climate change, CHARM is first run with rainfall data from 1960-1980 as a base case and then for average temperature increases of 1, 2, and 3 degrees Celsius and for precipitation changes of -30%, -15%, +15%, and +30%. The results of the sensitivity analysis are displayed in Figure 8:

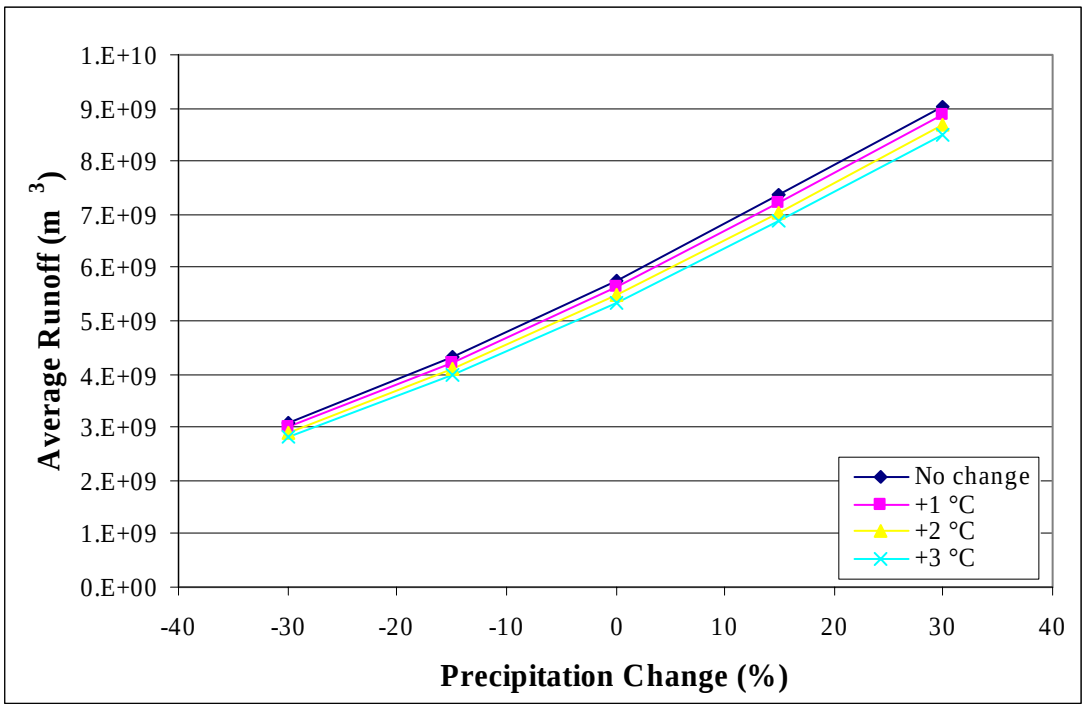

Figure 8: Climate sensitivity analysis in the Tao He

The figure shows that the sensitivity of annual runoff to temperature in the Tao He is small. Increased evapotranspiration decreases runoff by an average of 2.4% for each one-degree Celsius increase in temperature. Changes in precipitation naturally have a much larger effect. Increasing precipitation by 30% increases runoff by more than 50%, nearly twice as much.

4.1.4. Impacts of Climate Change on the Tao He

The results of simulating the Tao He with CHARM under six climate change scenarios from three general circulation models used by Working Group II in the Intergovernmental Panel on Climate Change's Second Assessment Report. The scenarios are transient, coupled ocean-atmosphere scenarios from the Geophysical Fluid Dynamics Laboratory's GFDL89 model (Manabe *et al.*, 1991, 1992), Max Plank Institute's ECHAM1-A (Cubasch *et al.*, 1992), and Hadley Center, UK's UKTR (Murphy *et al.* 1994, Murphy and Mitchell, 1994). The scenarios provide monthly temperature and precipitation values, under different emissions scenarios designed to represent the current and future situations. In this case, two time periods are used with decade two representing the years around 2020 and decade three representing years around 2050. Results of the climate change scenarios are then compared with a base climate developed from 30 years of historical data to produce monthly temperature differences and precipitation ratios between the base and changed-climate scenarios (Viner et. al., 1995). Table 3 below shows an overview of the annual temperature and precipitation changes predicted by the GCM scenarios for the Tao He basin. GF refers to the Geophysical Fluid Dynamics Laboratory's model scenarios, MP

refers to Max Plank Institute's model scenarios, HC refers to Hadley Center's model scenarios, TR refers to the fact that they are transient models, and 2 and 3 represent the decades modeled.

Tao He	GFTR2	GFTR3	MPTR2	MPTR3	HCTR2	HCTR3
Temperature change	2.27	3.03	1.81	2.88	1.27	2.79
Precipitation change	11.3%	18.0%	-2.0%	-0.2%	18.3%	18.7%

Table 3: GCM scenario output of annual temperature and precipitation change in the Tao He.

In all scenarios, temperature increases between one and four degrees Celsius. Precipitation, however, decreases in the Tao He under the ECHAM1-A scenarios, while it increases in all of the other scenarios. The GCM scenarios differ in how they distribute precipitation changes throughout the year, a fact that will be apparent in the CHARM simulation results.

The monthly temperature differences and precipitation ratios were input to CHARM to simulate runoff under the new climatic conditions. The results of these simulations are shown in Figure 9 and Figure 10.

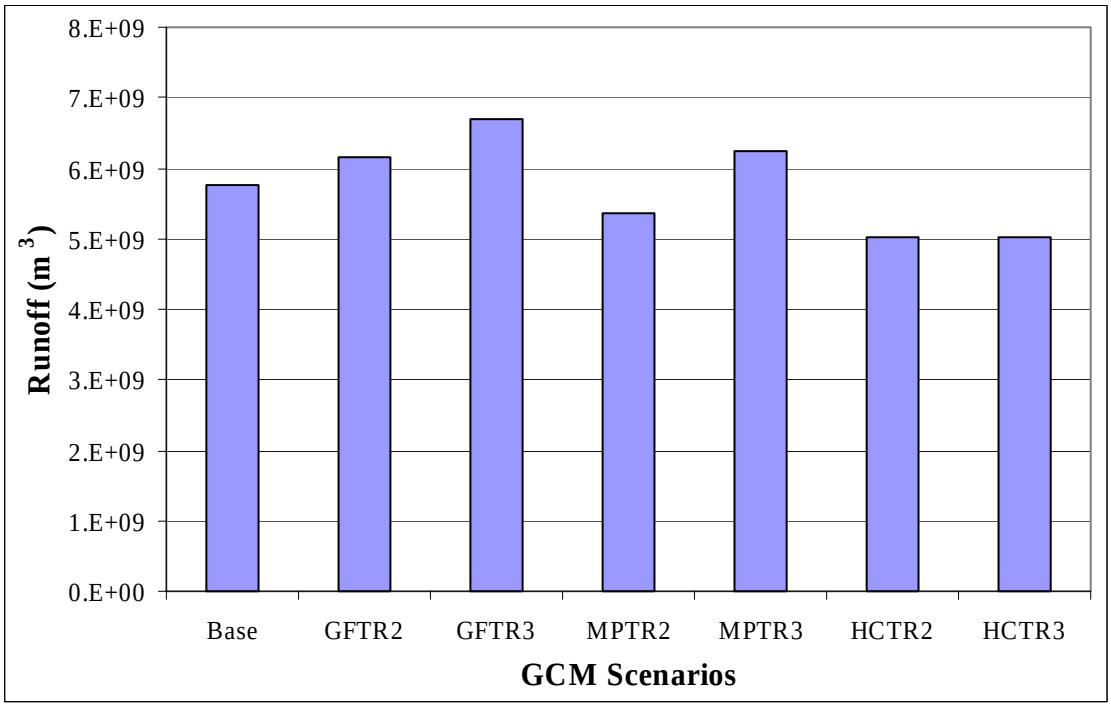

Figure 9: Results of climate change scenarios on annual runoff of the Tao He from three GCMs

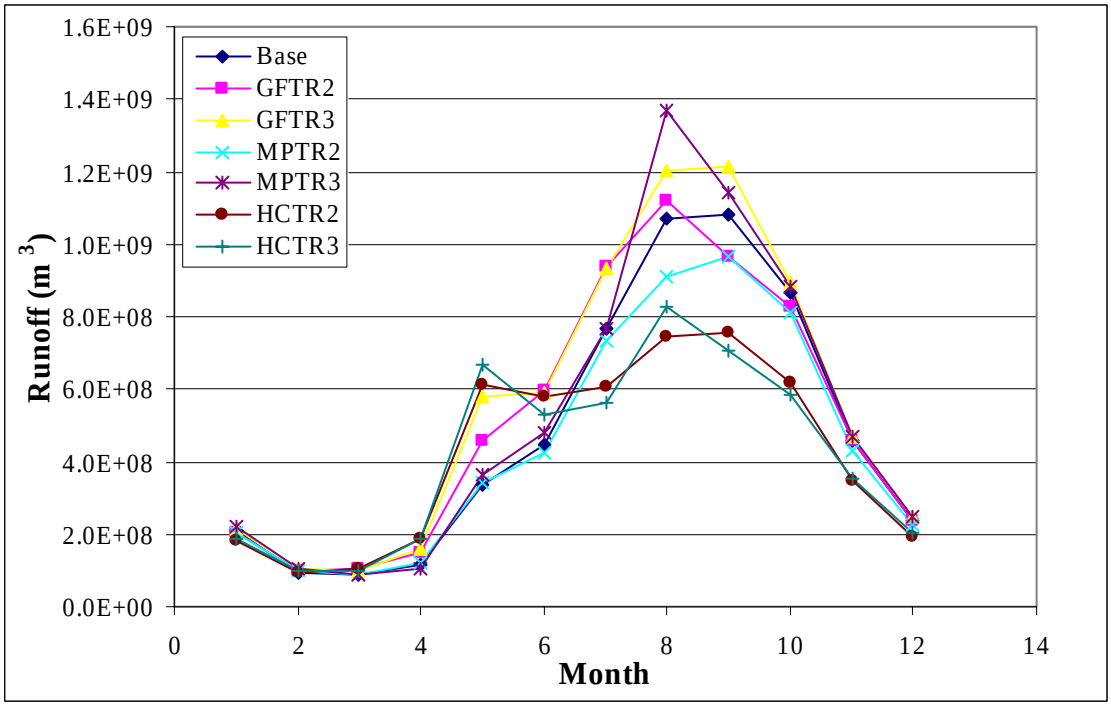

Figure 10: Results of climate change scenarios on monthly runoff of the Tao He

The GCMs do not agree as to how precipitation will change in the Tao He area, and hence differ on how runoff will be affected by climate change. The GFTR scenario for 2050 (GFTR3) predicts a 16% increase in runoff, while the HCTR scenario for the same decade produces a 13% decrease. These GCMs, however, do not model precipitation variables, as well as other climate variables, well at local scales such as a river basin (Howe and Henderson-Sellers, 1997; Viner et. al., 1995). An interesting result is that the changes in annual runoff are, in some cases, opposite in direction than changes in annual precipitation, due to changes in the timing of precipitation during the year. The Hadley scenarios, for instance, spread precipitation more evenly throughout the year, so that peak flows are not as high and more rain falls during dry periods when the soil can absorb and evaporate the additional moisture. The end result is less total runoff for the year, even though more precipitation actually fell. Figure 10 illustrates the result that not just the quantity of flow could change in the basin, but also the timing of flows. In three scenarios, the peak is actually shifted earlier in the year. The growing season for agriculture in the area could change as a result, or storage would have to be built to maintain the original hydrograph.

4.2. Yilou He

As another example of the testing and validation of CHARM, the results of calibrating and modeling the Yilou He are discussed here. The Yilou He is actually formed from two rivers, the Yi He and the Lou He, which originates in Shanxi province. For the purpose of this example the rivers will be grouped into one watershed and called the Yilou watershed. The watershed is about 400 km long and covers an area of approximately 20000 square kilometers. Located primarily in Henan province, it varies from an elevation of about 1700 meters at its highest to an altitude of about 100 meters as it flows into the Yellow River. It consists primarily of farmland, both irrigated and non-irrigated, but also has a substantial amount of timber forest and patches of hilly grassland and bush.

4.2.1. Calibration

As in the Tao He, runoff data for 1951 is available for the Yilou He, making this the best year to calibrate the model for the same reason as in the Tao He. The results of the calibration simulation for 1951 are shown in Figure 11:

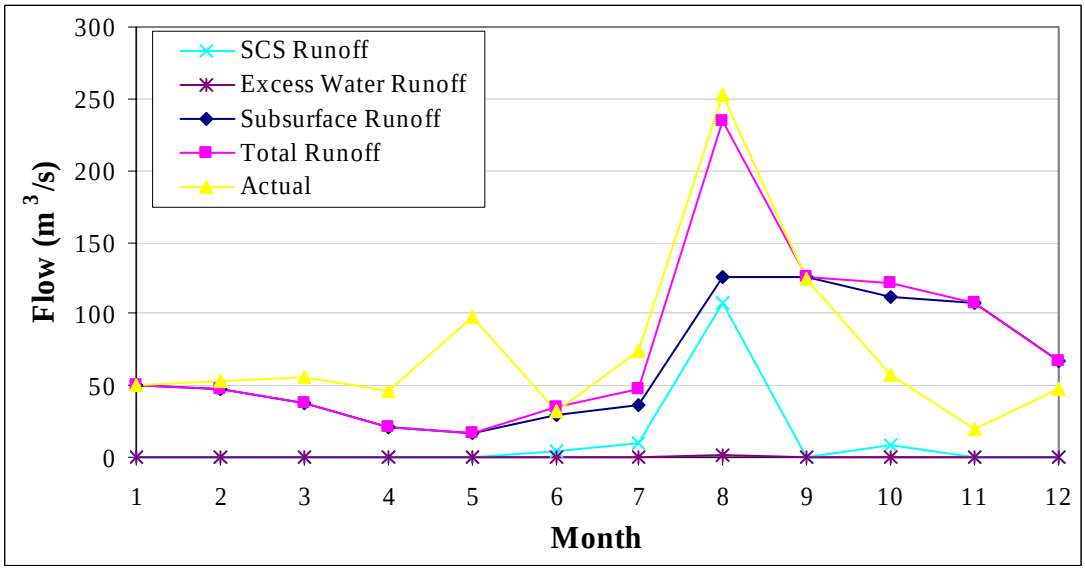

Figure 11: Comparison of actual with total simulated 1951 runoff and its components on the Yilou He.

In the case of the Yilou He for 1951, α calibrated to 3.9 and the difference between the actual and simulated annual runoff was about 4%. Figure 11 shows that the model matched the peak flow well, but the simulated flow declined at a slower rate than the actual runoff, suggesting that the model has more water retention in the soil and less direct surface runoff than is actually the case. The model also missed the first peak. However, there are many additional sources of error in modeling this basin as compared to modeling the Tao He. Like the Tao He, one major source of error is that daily rainfall data was only available at one rain gauge in the basin for 1951. Therefore the first peak could have resulted from a local storm that did not hit the rain gauge used for the simulation. Overall, the greatest source of error in modeling this basin is the development of irrigation and reservoirs. By 1960, seven completed reservoirs had a combined capacity of 1.24 billion cubic meters of storage, about 21% of the average annual flow, and many more reservoirs may have existed. The construction of these reservoirs combined with diversions for agriculture that started long before 1951 had a significant impact on the hydrograph downstream. The results of the modeling can only be viewed as the natural runoff that would occur if the rain gauge used was indicative of the rainfall over the entire basin.

After 1951, the next year of runoff data available for this study was 1971. By then, at least fifteen dams had been completed in the watershed. Three of them had just been completed and were filling while others were still under construction. By 1978, almost the entire average annual flow of the basin could be stored. Currently, close to 3 times the average annual flow can be stored. Trying to calibrate a rainfall/runoff model using raw stream flow measurements becomes futile without knowing more about the operational policy and releases from these reservoirs. The raw flow data now simply measures the releases from the reservoir upstream, which has many more reservoirs upstream of it. The stream flow data no longer necessarily has a simple and direct relationship to rainfall, but is determined by water management.

4.2.2. Sensitivity of the Yilou He to Land-Use and Climate Change

Figure 12 and Figure 13 illustrate the impacts of land-use change in the Yilou He, as measured by changing the SCS curve number.

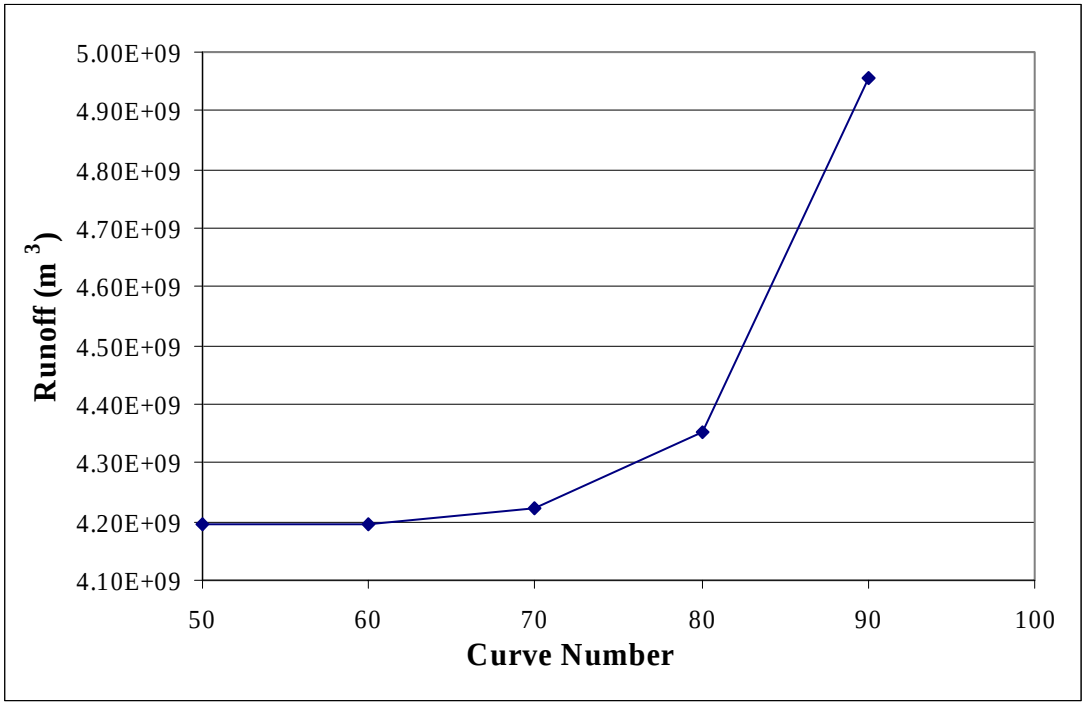

Figure 12: Sensitivity of annual runoff in the Yilou He to changes in the curve number

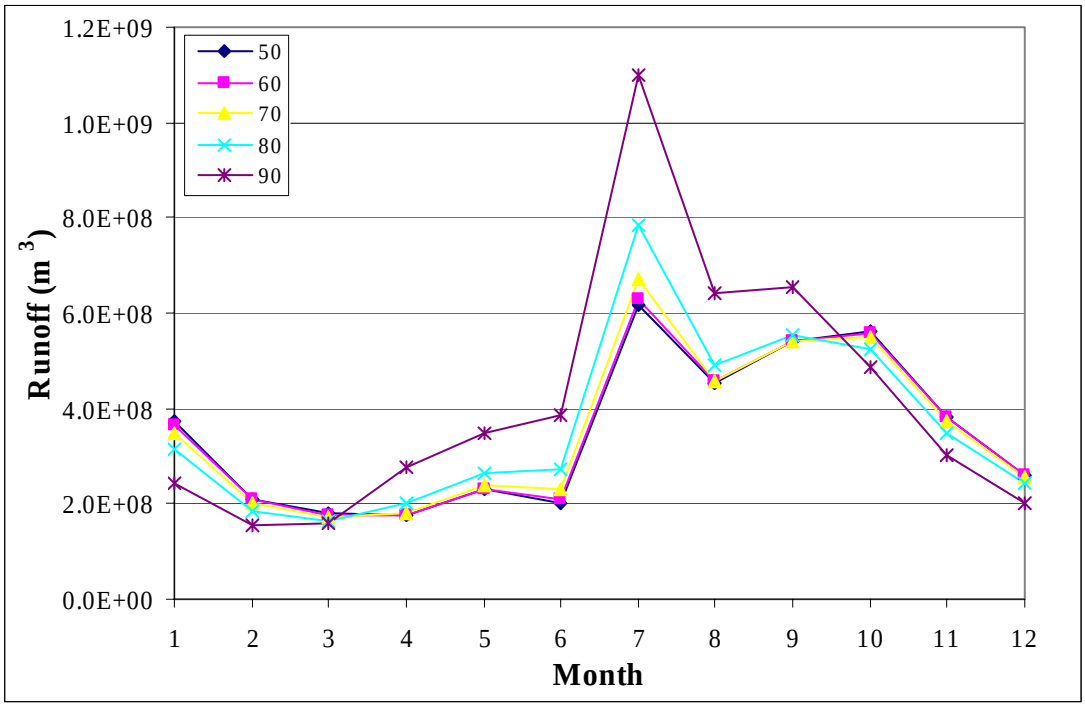

Figure 13: Sensitivity of monthly runoff in the Yilou He to changes in the curve number

In the Yilou He, the impact of land use change on runoff is more pronounced than in the Tae He, primarily because of the sharp peak runoff in July. Impermeable conditions cause even more of the intense rainfall during June through September to run directly off the land. In the Tao He, where the monthly hydrograph is smoother, annual runoff increased

only five percent between curve numbers of 50 and 90, but in the Yilou He the modeled increase is close to twenty percent. Flow in the peak month increased by an astounding 78%.

Sensitivity to temperature and precipitation change in the Yilou He, shown in Figure 14, is comparable to that on the Tao He. The sensitivity to precipitation changes is about the same as in the Tao He, whereas the temperature sensitivity is slightly higher at 3.4% per degree Celsius.

Table 3 below shows the annual temperature and precipitation changes predicted by the GCM scenarios for the Yilou He basin. In the Yilou He basin, all scenarios predict an increase in both temperature and precipitation.

Yilou He	gftr2	gftr3	mptr2	mptr3	hctr2	hctr3
Temperature change	2.88	3.79	2.06	2.99	1.21	2.45
Precipitation change	3.7%	12.1%	4.8%	9.0%	5.9%	11.8%

Table 4: GCM scenario output of annual temperature and precipitation change in the Yilou He.

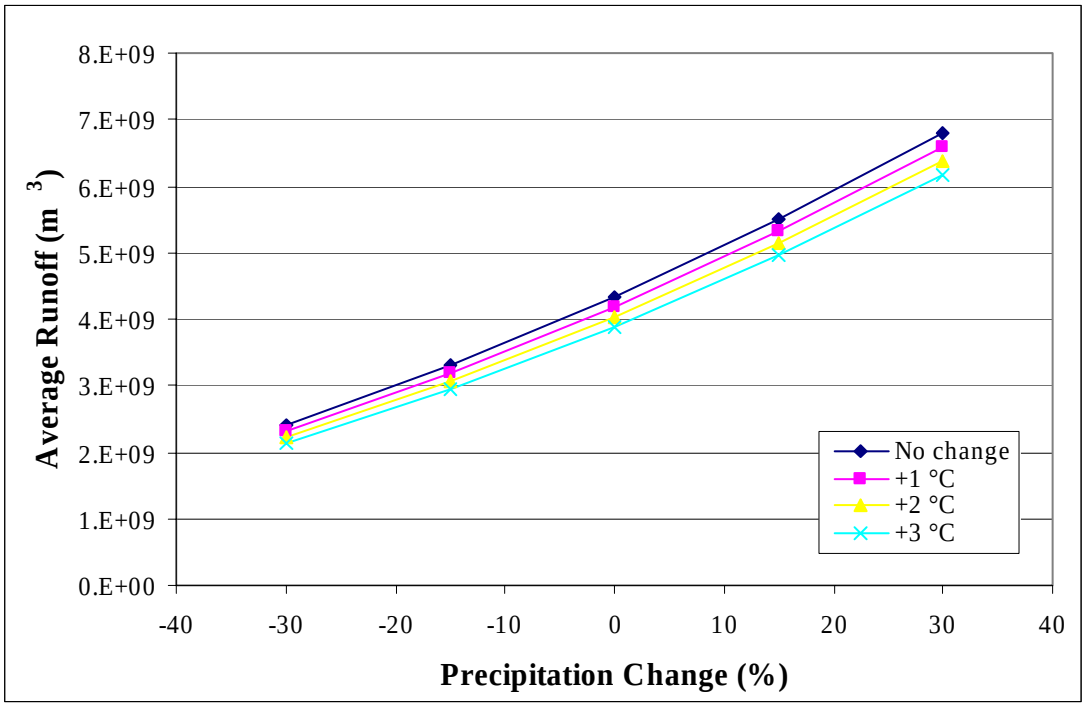

Figure 14: Climate sensitivity analysis in the Yilou He

Figure 15 and Figure 16 show the changes in annual and monthly runoff, respectively, under the GCM scenarios. Once again, the changes predicted by different GCM scenarios differ in both magnitude and direction. The changes, though, are substantial. At the extremes, the Hadley Scenario for the third decade (HCTR3) indicates an increase in runoff of over 30%, whereas the GFDL second decade shows a decrease of close to 25%. In HCTR3, the peak monthly flow increases by more than 75%.

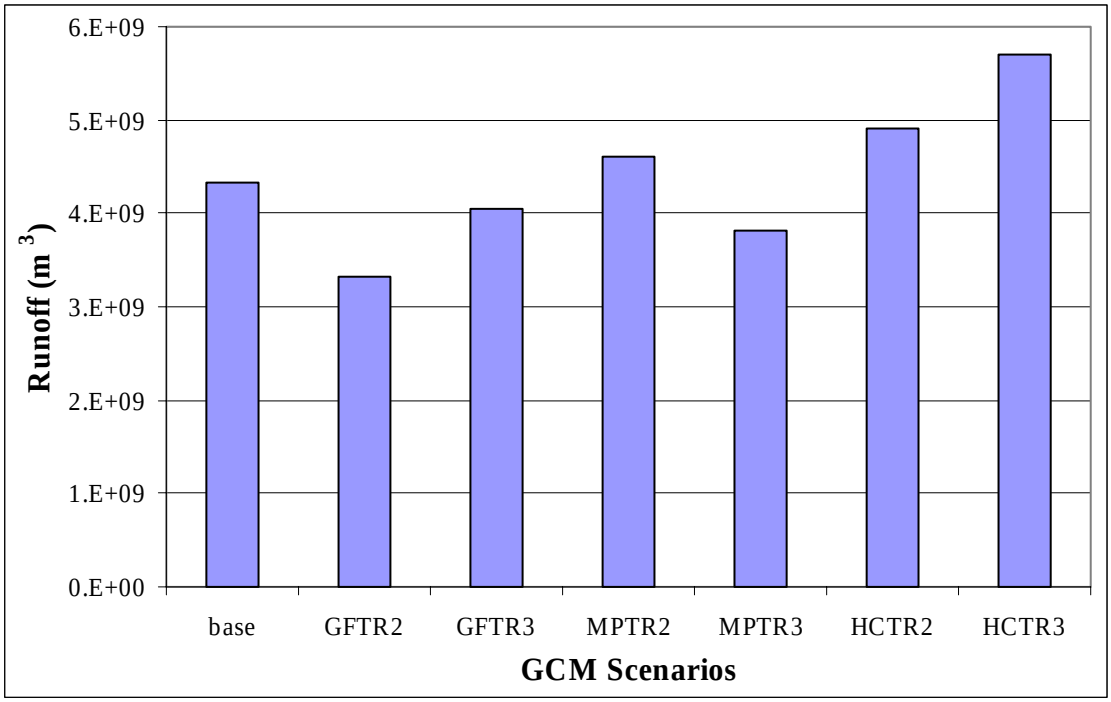

Figure 15: Results of climate change scenarios on annual runoff of the Yilou He from three GCMs

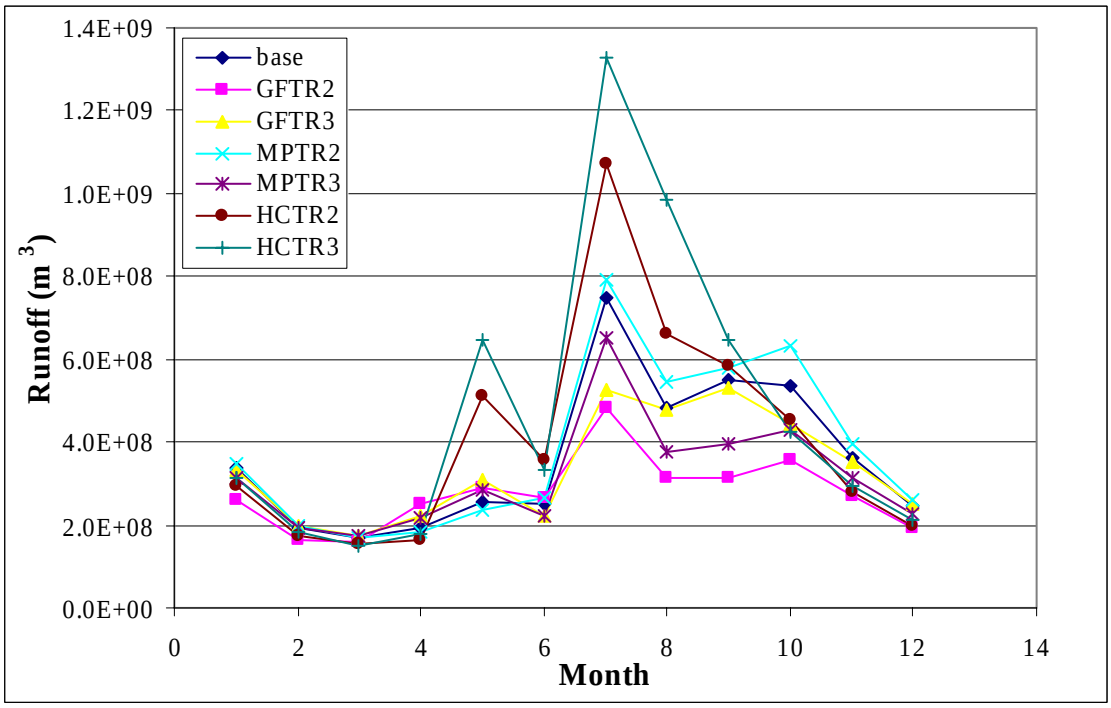

Figure 16: Results of climate change scenarios on monthly runoff of the Yilou He

4.3. Analysis of Land-Use and Climate Change on the Tao He and Yilou He

The land-use change figures for the Tao and Yilou He basins produce several important results. First, they show that different basins can react quite differently to changes in land-use, because of different geologic, geo-morphometric, and climatic conditions. Second, the figures show that land-use changes have a much smaller impact annually than they do intra-annually. Land-use changes have the effect of changing the timing of flows within the year, rather than making large changes in annual runoff, although significant changes

can also be made in annual flows. The runoff changes within a year usually produce more extreme events, greater peaks and longer droughts. Third, the more impermeable the land is made, the greater the impact of further land-use changes. Each of these results has repercussions for water management.

Figure 8 shows that the sensitivity of runoff to changes in average temperature in the Tao He is only about 2.4% per degree Celsius while runoff changes by an average of 1.72% for a 1% change in precipitation. Results were similar for the Yilou He where the sensitivity to average temperature was a bit greater at 3.4% per Celsius degree and runoff again changed 1.69% for a 1% change in precipitation. These results between the basins illustrate that different basins may react to climate change in different ways depending on the climatic and physical conditions of the basins. Figure 7 also shows that when increasing curve number, the peak flow of the Tao He moves earlier in the year, changing the hydrograph and perhaps presenting further challenges and expenses to water management in the watershed if the new hydrograph shape is less ideal. In the Yilou He the peak monthly flow remained in the same month.

Although the GCM scenarios show significant changes in the annual runoff for both the Tao and Yilou He, the different GCMs do not agree with each other on the magnitude or direction of these changes. In the Tao He, changes in precipitation in the second decade range from 6.8% for the GFTR to -12.8% for the HCTR. In the third decade, the GFTR predicts a 16.2% increase while the HCTR predicts a 13.1 percent decrease in runoff. Ranges in the Yilou He are similar, but directions are reversed. The GFTR predicts a 23.5% decrease in runoff for the first decade, while the HCTR predicts a 13.3% increase. In the third decade, the MPTR predicts the biggest decrease at 12.2%, while the HCTR predicts a 31.4% rise. Each of the GCM scenarios predicts a substantial change in runoff with the smallest changes being more than 6%. However, further conclusions cannot be drawn from these climate scenarios.

5. Discussion of CHARM Validation and Data Limitations

The examples of calibration and use of CHARM on the Tao He and Yilou He show that the model, which is calibrated to a yearly runoff value, also simulates monthly flows quite well. Because of heavy development in the Yilou He and in later years in the Tao He, the monthly runoff hydrograph has been significantly altered from the natural state calculated by CHARM. Smaller amounts of storage as seen in 1951 can affect the timing of flows significantly, but should not affect the total annual runoff much, so CHARM could still be calibrated to annual runoff at these basins in earlier years. Validating the model with monthly flows, though, is difficult since both of these watersheds were at least partially developed in the years that they could be modeled. The Tao He in 1951 was the least developed and so provides the best opportunity for model testing and validation.

The simulation for the Tao He basin matched the shape of the actual hydrograph reasonably well, but more and better data would result in more reliable parameterization of the model and improved simulations. Only one rain gauge was available with daily rainfall for the basin in 1951. The one flow gauge at the end of the basin provided only monthly average flows measured at the gauge, and other climatic data comes as monthly averages and not daily values. The benefits of more and better distributed rainfall data and data from more flow gauges in the basin are obvious. More rain gauges provide more accurate precipitation data and a better accounting of how much water is entering the region. More flow gauges with more frequent data would provide for better validation of the model and would enable routing components to be added to the model.

Slightly less obvious is how much help hydraulic soil parameters, which are not available, could be. As shown in Figures 4, 5, and 11, very little of the total simulated runoff is explained by the SCS curve number method for direct runoff. The majority of the runoff is from what the model describes as sub-surface runoff, which places a substantial burden on the calibration coefficient. Furthermore, in the model land-use change affects only the direct surface runoff. While in reality, land-use change may indeed have the greatest effect on the direct surface runoff; the sub-surface component could still be affected by increased or decreased hydraulic conductivity. This suggests that the α coefficient could also change slightly with land-use change, but the magnitude of this change is unknown. A few solutions to this problem are discussed below:

1. Detailed groundwater modeling may give more accurate results in the case of land-use change, but would also introduce many more parameters and unknowns into the system and require much more data.

2. Apply α coefficients for sub-surface runoff that correspond to different land-use, management, and soil types much like what is done with the curve numbers for direct surface runoff. In order to estimate such a set of land-use specific α coefficients, though, homogenous watersheds would have to be found that contain only one land-use and soil each. Estimations would need to be done for each land-use class, and data would need to be available accordingly.

Each of these solutions would add greater complexity to the model and require additional data. In the process, they may only result in small improvements to the simulations and are probably not justified for the primary use of the model. Some fine tuning improvements could be made to CHARM itself, such as adding a simple routing scheme and improving the modeling of transpiration changes throughout the year. These changes could be made

without more input data, but additional flow data would be required to validate the model's performance.

Ultimately, though, CHARM was designed to provide water availability estimates over large areas where detailed data is not always available. While the limitations of a model should be carefully considered when modeling and interpreting results, CHARM demonstrates that it is quite capable of approximating a complex system with limited data. Monthly flows in the less developed Tao He are well simulated. The calibration coefficient remains stable when calibrating the model for different years in the same basin, but varies slightly from basin to basin. This shows, as should be expected, that the calibration coefficient is a function of the physical features of the basin, such as the land-use and soil type. Finally, as shown in the previous section, CHARM is well suited to assessing the impacts of climate and land-use change on available surface water resources.

6. Assessing China's Water Supply and Demand Balance

Now that CHARM has been developed, tested, and validated, it is ready to be used to assess the surface water resources in China as a whole and the variability in the surface water supply. Knowledge of the surface water resources and their variability is essential to calculating how much water can be reliably supplied to different demands and how much investment must be made to use the available water efficiently and effectively.

A series of indexes, termed factors 1 to 5, is used to define and compare the water stress and security in major watershed regions in China. The first index is a per capita water resource scarcity index. It defines a condition of *water scarcity* when annual water supply is less than 1000 cubic meters per capita. *Water stress* is defined as between 1000 and 2000 cubic meters per capita. A second water stress index is related to water use, and defines *water stress* as a condition when the use/supply ratio is greater than 0.4. *Water surplus* is indicated by a use/supply ratio of less than 0.1. The third index is a measure of hydrologic variability. Higher variability results in higher risk. Here, a coefficient of variation of more than 0.3 is considered highly variable. Factor 4 is a risk reduction factor to indicate the extent to which current development has already reduced the risk from variability. If storage/annual flow is greater than 1, the supply risk from runoff variability is highly reduced. Combining the *Variability Factor* and the *Risk Reduction Factor* produces a *Water Resource Security Factor*, Factor 5. By assigning each category of each factor a number, a total water resource availability rating can be derived. Since Factors 3 and 4 are already combined to create Factor 5, only category values for Factors 1,2, and 5 are simply added to create this comprehensive *Water Resources Stress Index*. The following table summarizes the class ranges of these indexes.

Factor	*Category*	*Value*	*Description*
Factor1: Per Capita Water Scarcity Index[1] (Total Annual Renewable Water Resource/ Population)	0	> 2000 m^3/cap	Sufficient water
	1	1000 - 2000 m^3/cap	Water stress
	2	< 1000 m^3/cap	Water scarcity
Factor 2: Water Use Stress Index[2] (Use / Supply)	0	< 0.1	Water Surplus
	1	0.1 - 0.2	Sufficient water
	2	0.2 - 0.4	Moderate water stress
	3	> 0.4	Water Stress
Factor 3: Hydrologic Variability (Coefficient of Variation in annual runoff series)	0	< 0.1	Low variability
	1	0.1 - 0.2	Mild variability
	2	0.2 - 0.3	Variable
	3	> 0.3	High variability
Factor 4: Water Supply Risk Reduction (Storage / Annual Flow)	3	< 0.3	Limited reduction
	2	0.3 - 0.6	Mild Reduction
	1	0.6 - 1.0	Reduction
	0	> 1.0	High Reduction
Factor 5: Water Resource Security (Factor 3 category number + Factor 4 category number). This factor ranges from 0 - 6 with 0 being the most secure and 6, the least. The matrix in Table 6: Factor 5 is created by the combination of Factors 3 and 4. shows the tradeoff more clearly.			
Combined Water Resource Availability (Factor 1 + Factor 2 + Factor 5). This factor ranges from 0-11. As the number gets higher, the water resource situation gets worse. 0-3 very low stress, 4-5 low stress, 5-7, moderate stress, 7-8 high stress, 8-9 very high stress, 10-11 extremely high stress.			

Table 5: Indexes of water resource stress.

[1] Sandra Postel uses this as a scarcity index in her book *Last Oasis - Facing Water Scarcity*. She points to Malin Falkenmark, "The Massive Water Scarcity Now Threatening Africa - Why Isn't it Being Addressed?" *Ambio*, Vol. 20, No. 1, 1991. Shiklamonov (1993, 2000) arrives at a similar scarcity index by subtracting unrecoverable water consumption from total runoff and dividing by population. In Shiklamonov's grouping, < 1000 cubic meters per capita per year is considered catastrophically low, 1100 - 2000 is very low, 2100 - 5000 is low, 5100 - 10000 is average, 10100 - 20000 is high, and > 20000 is very high.

[2] Falkenmark and Lindh (1993) state that "Many countries, therefore, consider 30%-60% of theoretically available water resources to be the practical limit of what they can mobilize." They go on to say that 20% may be a better estimate in the short to medium term for developing countries, since costs of water development have become "…increasingly dominant in national economies" in the developed countries that have gone above this point. Raskin (1997) uses and explains the values used here.

Factor 5: Water Resource Security		***Factor 3: Hydrologic Variability***			
		0 - Low	**1 - Mild**	**2 – Variable**	**3 - High**
Factor 4: Water Supply Risk Reduction	**3 - Limited**	3 - Secure	4 - Mildly	5 – Mild	6 - Low
	2 - Mild	2 - Highly	3 - Secure	4 – Mild	5 - Mild
	1 - Reduction	1 - Highly	2 - Highly	3 – Secure	4 - Secure
	0 - High	0 - Highly	1 - Highly	2 – Highly	3 - Secure

Table 6: Factor 5 is created by the combination of Factors 3 and 4.

In order to calculate the surface water resources of China and the variability in the resource, the country was split into 9 major watershed regions for calibration with data from China's Ministry of Water Resources and Electric Power (UN, 1997). CHARM was then calibrated for each of these regions to the average annual runoff of the region. The results of simulating 1965-1980 are listed in Table 7 and displayed in Figure 17.

No.	Region	Observed Average Annual Runoff	Area	Modeled Results					
				Average Annual Runoff	Standard Deviation	Minimum	Maximum	Range	Average Annual Runoff Depth
		10^9 m^3	km^2	10^9 m^3	10^9 m^3	10^9 m^3	10^9 m^3	10^9 m^3	Mm
1	North-eastern	165.3	1242375	164.1	32.3	114.6	230.6	116.0	132.1
2	Hai He – Luan He Basin	28.8	297625	27.6	12.0	9.3	47.6	38.2	92.9
3	Huai He Basin	74.1	312050	75.7	24.7	44.6	126.8	82.2	242.7
4	Huang He Basin	66.1	841125	61.0	18.7	34.9	109.0	74.2	72.5
5	Chang Jiang Basin	951.3	1767980	938.3	113.1	755.8	1140.7	384.9	530.7
6	Southern	468.5	571400	440.7	86.6	298.7	601.7	303.1	771.2
7	South-eastern	255.7	199150	255.3	53.6	164.4	374.8	210.4	1281.7
8	South-western	585.3	816375	587.6	44.7	512.0	657.5	145.5	719.7
9	Interior Basins	116.4	3374750	113.1	11.6	92.4	134.5	42.1	33.5
	Total country	2712	9422830	2663	182	2451	3173	721	283

Table 7: Statistical results of calibrating and simulating CHARM for the nine watershed regions over years 1965-1980

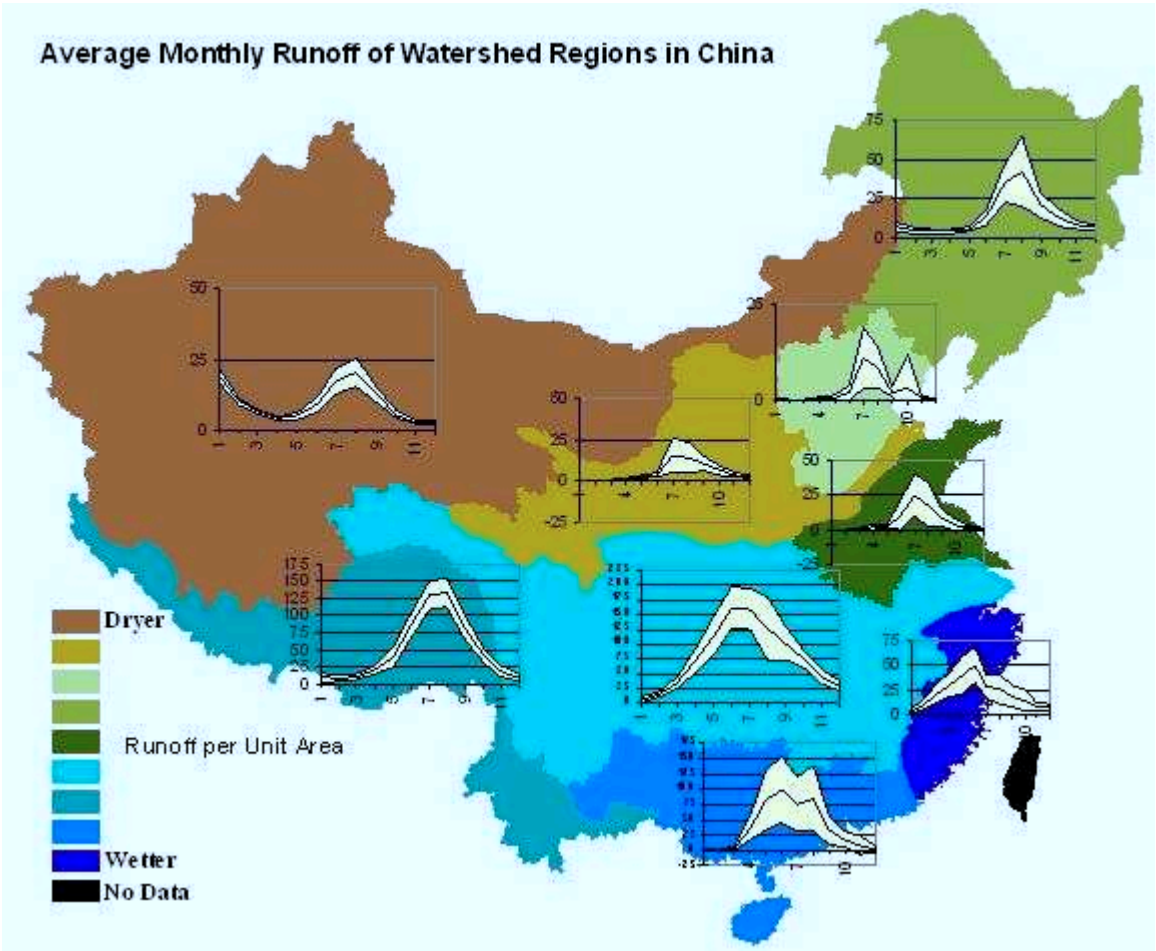

Figure 17: Map of the results of CHARM simulation for nine watershed regions over years 1965-1980. Each line on the charts represents 25 billion cubic meters. One standard deviation is plotted to either side of the mean monthly value.

Using the information garnered from CHARM, basin-specific stress indexes were calculated and are displayed in Table 9. Table 8 contains a summary of the data necessary to calculate the index values. The following sections discuss the regions and results in greater detail.

Regions	Supply	COV	Demand (1993)	Projected Demand (2000)	Projected Demand (2010)	Storage (10^9 m^3)	Population (millions)
1	164.1	0.20	51.93	66.31	87.07	52.4	111
2	27.6	0.43	46.47	50.36	57.29	22.1	105
3	75.7	0.33	73.46	86.83	105.09	11.8	192
4	61.0	0.31	44.95	49.91	63.41	41.5	111
5	938.3	0.12	196.53	224.46	261.45	167.4	391
6	440.7	0.20	77.19	93.13	121.17	71.3	131
7	255.3	0.21	32.09	39.04	47.37	38.2	76
8	587.6	0.08	8.37	10.09	12.39	17.0	16
9	113.1	0.10	62.13	68.26	78.45	43.5	22
National	2663.4	0.07	601.13	688.4	833.7	412.8	1155

Table 8: Summary of the data needed to calculate the water resources factors described in Table 5.[3]

	Factor 1 Population		Factor 2 - Use						Factor 3 COV		Factor 4 Storage		Factor 5 Security	Factor 6		
			1993		2000		2010							93	00	10
1	1	1473	2	0.32	2	0.40	3	0.53	1	0.20	2	0.32	3	6	6	7
2	2	264	3	1.68	3	1.82	3	2.07	3	0.43	1	0.80	4	9	9	9
3	2	395	3	0.97	3	1.15	3	1.39	2	0.33	3	0.16	5	10	10	10
4	2	551	3	0.74	3	0.82	3	1.04	2	0.31	1	0.68	3	8	8	8
5	0	2403	2	0.21	2	0.24	2	0.28	1	0.12	3	0.18	4	6	6	6
6	0	3358	1	0.18	2	0.21	2	0.27	1	0.20	3	0.16	4	5	6	6
7	0	3346	1	0.13	1	0.15	1	0.19	2	0.21	3	0.15	5	6	6	6
8	0	35850	0	0.01	0	0.02	0	0.02	0	0.08	3	0.03	3	3	3	3
9	0	5172	3	0.55	3	0.60	3	0.69	0	0.10	2	0.38	2	5	5	5
N	0	2306	2	0.23	2	0.26	2	0.31	0	0.07	3	0.17	3	5	5	5

Table 9: Water stress factors and values of index calculations for major watershed regions of China.

6.1. General China Issues

Table 9 and Figure 17 show that surface-water runoff varies considerably among the different regions and also between years. Modeled runoff is within 2% of observed for the entire country. The interior basins, by far the driest, produce only 34 mm of runoff throughout the area, whereas the Southeast produces nearly 40 times as much. Three of the

[3] The supply and coefficient of variation came from simulation with CHARM. Demand values and projections taken from UN (1997). Storage values were obtained from ICOLD (1984), and from personal correspondence with the Institute of Geography of the Chinese Academy of Sciences. Finally, population was taken from the 1992 China Statistical Yearbook.

nine basins do not have the surface water resources to meet projected demand in 2010. If demand grows at the projected rate, water will have to be transferred from southern basins in order to meet demand in the northern part of the densely populated North-China Plain.

The inter-annual variation is also significant. On average, the minimum annual flow for these 16 years is 40% below the average runoff. In regions that have water shortages, enough storage must be built to hold more than an entire year's runoff in order to reliably supply water over many years.

Not shown in Table 9 is the variation within the year. This variability is illustrated in Figure 17. The figure clearly shows that in almost all of the watersheds, 60% of the runoff occurs during only three months of the year, with the remaining months being left quite dry. This high variability in both seasonal and annual flows is what led to the construction of more than 83,000 dams in China by 1990 (UN, 1997). In the following sections, we summarize the key features of each of the nine watershed regions and for each, discuss the simulation results previously presented in Table 9.

6.2. The Northeast

The Northeast region contains several major rivers including the Heilong Jiang (Amur), Songhua (Sungari), Wusuli (Ussuri), Liao He, Yalu, and Tumen. The region covers approximately 13% of the total area of China, or about 1.25 million square kilometers, and contains about 10% of the population but only produces 6% of China's surface water runoff. The per-capita surface-water runoff of 1000 cubic meters per person per year is below China's national average of 2300 cubic meters per person per year and is an indication of water stress.

The three major land-uses in the region are timber forest, non-irrigated farmland and grassland. Together, these account for 85% of the area. The average runoff per unit area, 132 mm, is currently sufficient for these uses. However, additional irrigation is planned for the region with demand for irrigation water increasing by 20% between 2000 and 2010. The value of the combined water stress index is in the middle of its range at 6, but the water stress increases with increasing demand by 2010, when the index value moves to 7. The factors all indicate stressed water resources in the region. However, with further expansion and improvement of water infrastructure, enough water does exist in the region to satisfy basic needs.

6.3. Hai He – Luan He Basin

The Hai He – Luan He Basin presents major challenges to water resource management in China. The region is significantly smaller, at only 3.4% of the total area of China, than the Northeast, but has a much greater population, more than 9% of the total population of China. This results in a per-capita surface water availability of only 264 cubic meters per capita per year. This certainly indicates a region of considerable water stress. The scarcity is exacerbated not only by a large population, but also by land-use and high rainfall, and therefore runoff, variability. More than 25% of the total area in the region is irrigated farmland, which accounts for two-thirds of the water use or the entire surface runoff produced in the region on average. Another 30% is non-irrigated farmland. Total water use in the region for 1993 was estimated to be 41 billion cubic meters, significantly larger than the 28 billion cubic meters of runoff produced in the region for that year. Furthermore,

water demand in the region is expected to reach 57 billion cubic meters by 2010. Groundwater has been used to bridge the gap between supply and demand in the region. However, this use cannot be sustained, as groundwater table levels have been dropping by 1-2 meters per year.

The CHARM modeling exercise illustrates the additional problem of high runoff variability in the region. Although the per capita annual surface water runoff is 264 cubic meters on average, the lowest runoff in the 15 simulated years is only 9 billion cubic meters total or 89 cubic meters per capita. Intra-annual variability is also a concern, since nearly all the rainfall and runoff, 87% on average, occurs between July and October. Storage has been and continues to be built to reduce the variability in supply. In fact, only the large storage capacity built in the region to reduce water-supply variability keeps the combined stress index of 9 below that of the Huai basin, but Factors 1, 2, and 3 assume the worst values of all regions in China with demand not being met by average runoff in the region. Furthermore, due to evaporation, seepage and other losses, not even the average runoff can be delivered to where it is needed. This is a region of extremely high water stress that must import water to meet its needs.

6.4. Huai He Basin

The Huai He Basin has much in common with the Hai He – Luan He Basin, also covering 3.5% of the nations area and containing a large percentage of the population, in this case 17%. The region also contains some of the country's best arable land. The population is larger in the Hai He basin, but so is the runoff. At 395 cubic meters per capita runoff is actually 50% higher than in the Huai He – Luan He, but the region is still water-scarce. In this basin, irrigated farmland is the primary land-use, accounting for 31% of the area. Timber forest, paddy, and non-irrigated farmland are the other major land-uses. Once again, demand is expected to outstrip surface water supply in 2010, with demand reaching 105 billion cubic meters, while average annual surface water supply is about 75 billion cubic meters.

As in the Hai He – Luan He Basin and as shown in Table 9 and Figure 17, the Huai He Basin suffers from great variability in runoff. Modeled flows range from 45 to 127 billion cubic meters per year, with 87% of the runoff between June and October.

6.5. Huang He Basin

The Huang He, or Yellow River, is the second longest river in China, being exceeded in length only by the Chang Jiang (Yangtze). However, at 60 billion cubic meters per year, the Huang He carries only 7% of the Yangtze's annual runoff. Since the Huang He Basin is more arid than the Chang Jiang Basin, the variability of rainfall and runoff is also much greater. In a low year, the Huang He Basin may produce only 50% of the surface water runoff of an average year. The flow is highly seasonal, with 77% between July and October, and only 1% of annual flow combined for January, February, and March. Since the entire volume of flow in these months has been diverted and used in recent years, the Huang He does not even flow to the sea in this period each year and sometimes for even a longer period stretching into April and May.

The total area of the Huang He Basin, about 8% of the country, is less than that of the Northeast, but the population is about the same. Per capita annual surface water runoff is

550 cubic meters, still well within the water scarce range. Major land-uses in the region include steppe grassland, 41% of the area, non-irrigated farmland, 17%, irrigated farmland, 13%, and mountainous grassland, 12%.

By 2010, demand for water will outstrip average surface water runoff by 4%. Compared to Hai He-Luan He and Huai He Basins, 4% is not so much. However, the Yellow River presents additional challenges to water management. The river obtained its name, Yellow River, from the huge quantities, 1.6 billion tons per year, of yellow silt eroded from the Loess Plateau and carried by the river. Silt quickly fills the many reservoirs built on the river and diminishes their storage capacity. For instance, begun in the late 1950s, "…Yangouxia Dam lost almost one-third of its storage capacity before it was even commissioned. By 1966, three-quarters of Yangouxia's reservoir had been filled with sediment." (McCully, 1996, p. 108)

6.6. Chang Jiang Basin

The Chang Jiang, or Yangtze, is China's largest river. The basin covers 19% of the country and carries 35% of the surface runoff. Per capita annual runoff is 2,400 cubic meters. Due to the plentiful precipitation, irrigated dryland agriculture accounts for only a very small percentage of the land-use in this region. Paddies, however, cover some 16% of the area. Timber forest covers the greatest area, 28%, while non-irrigated farmland, 11%, mountainous grassland, 11%, steppe, 15%, and brush, 10%, makes up much of the rest of the area.

The Chang Jiang has produced some of China's most disastrous floods because of the volume of water it carries. In 1931, for instance, 3.3 million hectares of farmland were inundated, 140,000 people drowned and 3 million people were rendered homeless (Dakang and Yan, 1992). However, the coefficient of variation in annual flows is low compared to the basins in the northern part of the country. The result is that even in years of low runoff, water demand in the basin can easily be met. This, in turn, has made the basin a good candidate for water transfers to basins in the North, where demand is not being met. Several options for water transfers to the North are under consideration, with one, following the route of the ancient Grand Canal in the east, already beginning to be implemented.

6.7. Southern

The southern watershed region is quite mountainous, with 17% of the area covered by mountainous grassland and 30 % by timber forest. The basin is strongly affected by monsoons and the moisture from the South China Sea, producing the second largest runoff depth, close to 800 mm per year, and per-capita runoff, 3300 cubic meters, of the nine watershed regions. The sub-tropical/tropical climate and high runoff makes the area suitable to grow rice, which is done over 18% of the area. Non-irrigated farmland makes up another 10% of the region.

The variability in this region is greater than in the Chang Jiang Basin. As in the case of the Chang Jiang, though, water demand can be met by surface water runoff even in low-flow years. As with much of China, though, the flow can vary greatly within a year with only 1% produced from January through March. For this reason, storage and irrigation may be necessary to grow crops in these months.

6.8. South-eastern

The South-eastern region is 57% forest and 28% paddy. It is the smallest of the watershed regions covering only 2.4% of the country, but has a higher population density than any other region, except the Hai He-Luan He Basin. Like all of the regions in the southern half of the country, the South-east has more than enough water. Per capita surface runoff is almost equal to that in the Southern watershed region, and average runoff depth even higher at over 1000 mm per year.

6.9. South-western

The South-western watershed region, including major rivers originating from the Tibetan Plateau, is composed almost entirely of high altitude prairie, forest, and bare land. The runoff depth is not the greatest in the southern half of China, but because of the very low population density in the region, the per capita runoff is by far the greatest of any region at 36000 cubic meters per capita. The region also has the smallest inter-annual variability. The high precipitation, low variability, and low demand in the region insure that water shortages will not occur here.

6.10. Interior basins

The largest watershed region in China, covering 35% of the country, contains no rivers that flow to the sea. The Interior Basins are extremely arid with an annual average of only 34 mm of runoff over an entire region that is 16% desert, 9% Gobi, 50% steppe, and 12% bare land. It receives only 4% of China's total annual runoff but still contains irrigated land on 2% of its area. The population of the region is also very small, amounting to only 2% of China's total population. This, in turn, results in a higher per capita runoff, 5000 cubic meters, than the heavily populated basins farther east. Because water demand has been very low, the demand can currently be met by surface water supply in the region.

7. Conclusions

CHARM is a rainfall-runoff model designed to be as simple as possible for use in assessing the effects of land-use and climate change on water resources in China, subject to limited availability of data for model calibration and validation. After first calculating the direct surface runoff, CHARM performs a water balance on the remaining water that does not immediately run off but infiltrates into the soil. Evapotranspiration and sub-surface runoff remove water from the soil. If the soil is saturated, any additional water runs off over the surface. Changing land-use affects CHARM by changing the volume of water that runs off as direct surface runoff. Climate change effects can be modeled by changing the precipitation, temperature, and radiation inputs to the model, which affect all components of the model.

The calibration and modeling of several sample basins, such as the Tao He and Yilou He, produced good results and also showed some challenges and areas where the model could be improved. Once calibrated, CHARM performed well in modeling both of these basins, tracking especially well for years prior to massive dam construction. As requested in the control input, the model calibrated within 5% to the annual runoff in both cases, also approximating the shape of the monthly hydrograph, even without using explicit routing calculations. For the Yilou He, the simulated runoff did not drop quite as quickly after the summer peak as the actual runoff did, suggesting that the model may underestimate direct runoff and overestimate water retention in the soil in this particular region. The simulation also missed a small runoff peak in May, which could have come from a local storm near a rain gauge with no 1951 data. Another possibility is that dams already existed in the river, which would explain both of these differences. The other interesting conclusion from the sample basins is that direct surface runoff is a relatively small portion of the total simulated runoff. Since the direct runoff is the component that is sensitive to land-use changes, this may indicate that changes in runoff due to changes in land-use are small. Furthermore, the calibration coefficient, α, and therefore sub-surface runoff could also change with land-use, but the nature of this relationship is still unknown. The effects of land-use change on water resources, therefore, may be underestimated by CHARM.

CHARM provides a means of calculating the amount of surface water resources and the variability in the surface water resources in China. The average amount of the surface water resources is certainly an important characteristic of the water sector and already shows that water shortage is a problem in some areas. If receiving less than 2740 liters per person per day is considered water scarce (Postel, 1992), then at least three of the nine watershed regions in China are water scarce, even if all of the average surface water runoff could be considered water supply. However, the average runoff cannot be delivered consistently as water supply and there is considerable variability in the runoff, which poses an even greater challenge to water managers. Variability can be simulated by CHARM by first calibrating large regions in China to actual data. Then runoff can be calculated by CHARM for different years based on the climatic inputs. The simulations provide information about the variability of runoff in China, which is needed for efficient management of water resources.

Runoff does indeed prove quite variable in both time and space. The Northwest interior produces only about 34 mm of runoff annually on average, whereas the Southeast produces over 1200 mm. Inter-annually, the variation is also significant, with the coefficient of variation as high as 0.4. Within the year, 60% of the runoff in almost all basins arrives in only three months. This variability in runoff is one of the major problems faced by water resource managers who need steady resource supplies. The simulation

results obtained with CHARM show that China is facing serious water supply problems, which most likely will worsen in the future with a growing population. Land-use change and climate change could exacerbate or help mediate the variability of runoff. CHARM provides a tool to aid in measuring these effects in future studies.

References

Bowling, Perrin and Kenneth Strzepek. 1997. *Examining the impacts of land use change on hydrologic resources*. IIASA Interim Report, IR-97-31, Laxenburg, Austria.

Gao, Songfan, Yang Qinye and Lu Qi, 1992. "The Changjiang Valley," in *The Natural Features of China*, Chinese Academy of Sciences, Institute of Geography, Eds. Zuo Dakang and Xing Yan, China Pictorial Publishing House, Beijing.

Chow, Ven Te, David R. Maidment, Larry W. Mays, 1988. *Applied Hydrology*. McGraw-Hill, New York.

Cubasch, U., K. Hasselmann, H. Hock, E. Maier-Reimer, U. Mikolajewicz, B. D. Santer, and R. Sausen, 1992. "Time-Dependent greenhouse warming computations with a coupled ocean-atmosphere model," *Climate Dynamics* **8**, pp. 55-69.

EPA, 1994. *The Hydrologic Evaluation of Landfill Performance (HELP) Model*. Risk Reduction Engineering Laboratory, Office of Research and Development, USEPA, Cincinnati, Ohio.

Falkenmark, Malin and Gunnar Lindh, 1993. "Water and Economic Development," in in Water in Crisis - A Guide to the World's Fresh Water Resources. Ed. Peter H. Gleick. Oxford University Press, New York.

FAO, 1998. Allen, Richard G., Luis S. Pereira, Dirk Raes, and Martin Smith: *Crop Evapotranspiration – Guidelines for Computing Corp Water Requirements; FAO Irrigation and Drainage Paper 56*. FAO, Rome.

Fischer, Günther, Harrij van Velthuizen, and Freddy O. Nachtergaele, 2000. *Global Agro-Ecological Zones Assessment: Methodology and Results*. IIASA Interim Report, IR-00-064, Laxenburg, Austria.

Greco, Steven, Richard H. Moss, David Viner, and Roy Jenne, 1994. Climate Scenarios and Socioeconomic Projections for IPCC WG II ASSESSMENT, CIESIN.

Howe, Wendy and Ann Henderson-Sellers, 1997. *Assessing Climate Change : Results from the Model Evaluation Consortium for Climate Assessment*. G & B Science Pub; ISBN: 9056990675.

ICOLD, 1984. *World Register of Dams*. International Commission on Large Dams, Paris.

Kaczmarek, Z. and D. Krasuski, 1991. *Sensitivity of Water Balance to Climate Change and Variability*, IIASA Working Paper, WP-91-047, Laxenburg, Austria.

Manabe, S., R. J. Stouffer, M. J. Spelman, and K. Bryan, 1991. "Transient Responses of a Coupled Ocean-Atmosphere Model to Gradual Changes of Atmospheric CO_2. Part 1: Annual Mean Response," *J. of Climate* **4**, 785-818.

Manabe, S., M. J. Spelman, and R. J. Stouffer, 1992. "Transient Responses of a Coupled Ocean-Atmosphere Model to Gradual Changes of Atmospheric CO_2. Part 2: Seasonal response," *J. of Climate* **5**, 105-126.

McCully, Patrick, 1996. *Silenced Rivers – The Ecology and Politics of Large Dams*, Zed Books, London and New Jersey.

Murphy, J. M., 1995. "Transient Response of the Hadley Centre Coupled Ocean-Atmosphere Model to Increasing Carbon Dioxide. Part I: Control Climate and Flux Adjustment," *J. of Climate* **8**, 36-56.

Murphy, J. M. and J. F. B. Mitchell, 1995. "Transient Response of the Hadley Centre Coupled Ocean-Atmosphere Model to Increasing Carbon Dioxide. Part II: Spatial and Temporal Structure of the Response," *J. of Climate* **8**, 57-80.

Nanjing Institute of Hydrology and Water Resources, *Report on the mid- and long-term plans for water demand and supply in China*, 1996.

Postal, Sandra, 1992. Last Oasis, Facing Water Scarcity. W.W. Norton & Company, New York.

Press, William H., Saul A. Teukolsky, William T. Vetterling, and Brian P. Flannery, 1992. *Numerical Recipes in C: The Art of Scientific Computing Second Edition*. Cambridge University Press, New York.

Raskin, P., P. Gleick, P. Kirshen, G. Pontius, and K. Strzepek, 1997. Water Rutures: Assessment of Long-range Patterns and Problems. Background Document for the SEI/United Nations Comprehensive Assessment of the Freshwater Resources of the World. Stockholm: Stockholm Environment Institute.

Shiklamanov, Igor, 1993. "World Fresh Water Resources," in Water in Crisis - A Guide to the World's Fresh Water Resources. Ed. Peter H. Gleick. Oxford University Press, New York.

Shiklamanov, Igor, 2000. "World Water Resources and Water Use: Present Assessment and Outlook for 2025," in *World Water Scenarios: Analysis.* World Water Vision, http://www.watervision.org.

Smith, Martin. 1992. CROPWAT, a computer program for irrigation planning and management, *Irrigation and Drainage Paper 46*, U.N. Food and Agriculture Organization, Rome, Italy.

UN, 1997. *Study on Assessment of Water Resources of Member Countries and Demand by User Sectors: China: Water Resources and Their Use*. United Nations, New York.

USDA, Soil Conservation Service. 1985. *National Engineering Handbook, Section 4, Hydrology*. US Government Printing Office, Washington, D.C.

USDA, 1986. Urban Hydrology for Small Watersheds. Engineering Division, Soil Conservation Service, USDA, Technical Release 55.

USDA, 1994. *SWAT Soil and Water Assessment Tool*. Agricultural Research Service, Grassland, Soil and Water Research Laboratory, USDA, Temple, Texas.

Viner, D., M. Hulme and S.C.B. Raper, 1995. Climate Change Scenarios for the IPCC Working Group II Impacts Assessment: Technical Note No. 6. Climatic Research Unit, School of Environmental Sciences, University of East Anglia, Norwich.

Yates, D. 1996. WatBal-An Integrated Water Balance Model for Climate Impact Assessment of River Basin Runoff. *Water Resources Development* 12(2):121-39.

Appendix I: Calculation of Evapotranspiration

The first step in calculating evapotranspiration is to calculate the reference evapotranspiration (ET_0). Reference evapotranspiration in CHARM follows the Penman-Monteith method as recommended by FAO (FAO, 1992; 1998), the same method that the LUC project uses for the agro-ecological zoning methodology (Fischer *et al.*, 2000). The Penman-Monteith equation can be written as:

$$ET_0 = ET_{ar} + ET_{ra} \qquad \textbf{Equation 11}$$

where ET_{ar} is the aerodynamic term or:

$$ET_{ar} = \frac{\gamma}{\upsilon + \gamma^*} \cdot \frac{900}{T_a + 273} \cdot U2 \cdot (e_a - e_d) \qquad \textbf{Equation 12}$$

and ET_{ra} is the radiation term or:

$$ET_{ra} = \frac{\upsilon}{\upsilon + \gamma^*} \cdot (R_n - G) \cdot \frac{1}{\lambda} \qquad \textbf{Equation 13}$$

and

γ ≡ psychrometric constant (kPa/°C)

γ^* ≡ modified psychrometric constant (kPa/°C)

ν ≡ slope vapor pressure curve (kPa/°C)

T_a ≡ average daily temperature (°C)

e_a ≡ saturation vapor pressure (kPa)

e_d ≡ vapor pressure at dew point (kPa)

$e_d - e_a$ ≡ vapor pressure deficit (kPa)

U2 ≡ wind speed (m/s)

R_n ≡ net radiation flux at surface (MJ/m^{2}d)

G ≡ soil heat flux (MJ/m^{2}d)

λ ≡ latent heat of vaporization (MJ/kg)

The calculation of the variables listed above is done as follows:

Average daily temperature (°C)

$$T_a = 0.5(T_{\max} + T_{\min}) \qquad \textbf{Equation 14}$$

where T_{min} and T_{max} are the maximum and minimum daily temperatures, respectively, and are given as inputs.

Latent heat of vaporization (MJ/kg)

$$\lambda = 2.501 - 0.002361 T_a$$ **Equation 15**

Psychrometric constant (kPa/°C)

$$\gamma = 0.0016286 \cdot \frac{P}{\lambda}$$ **Equation 16**

where the atmospheric pressure (P) at elevation (A), given as input, is calculated by the following equation:

$$P = 101.3\left(\frac{293 - 0.0065A}{293}\right)^{5.256}$$ **Equation 17**

Modified psychrometric constant (kPa/°C)

$$\gamma^* = \gamma\left(1 + \frac{r_c}{r_a}\right)$$ **Equation 18**

r_a is the aerodynamic resistance defined by:

$$r_a = \frac{208}{U2}$$ **Equation 19**

where U2 is the wind speed (m/s) which is input to the program. r_c is the crop canopy resistance:

$$r_c = \frac{R_l}{0.5LAI}$$ **Equation 20**

and LAI is the leaf area index assumed to be 2.88.

Saturation vapor pressure (kPa)

$$e_a = 0.5(e_{ax} + e_{an})$$ **Equation 21**

$$e_{ax} = 0.6108 \exp\left(\frac{17.27 T_{\max}}{237.3 + T_{\max}}\right)$$ **Equation 22**

$$e_{an} = 0.6108 \exp\left(\frac{17.27 T_{\min}}{237.3 + T_{\min}}\right)$$ **Equation 23**

Dew point vapor pressure (kPa)

$$e_d = \frac{RH}{100} \cdot \frac{0.5}{\left(\frac{1}{e_{ax}} + \frac{1}{e_{an}}\right)}$$ **Equation 24**

Relative Humidity (RH) is given as an input or calculated by the following regression:

Slope of the vapor pressure curve (kPa/°C)

$$e_a = 0.5(\upsilon_x + \upsilon_n)$$ **Equation 25**

where:

$$\upsilon_x = \frac{4096 e_{ax}}{(237.3 + T_{\max})^2}$$ **Equation 26**

$$\upsilon_n = \frac{4096 e_{an}}{(237.3 + T_{\min})^2}$$ **Equation 27**

Net radiation flux at surface (MJ/m^{2}d)

$$R_n = R_{ns} - R_{nl}$$ **Equation 28**

Here, R_{ns} is the net incoming shortwave radiation and R_{nl} is the net outgoing longwave radiation. The shortwave radiation term will be developed first followed by the longwave term:

Net incoming short-wave radiation (MJ/m^{2}d)

For a reference crop with assumed albedo coefficient α=0.23:

$$R_{ns} = 0.77 R_s$$ **Equation 29**

and the short-wave radiation (R_s) is:

$$R_s = \left(.25 + .5\frac{SD}{DL}\right) R_a$$ **Equation 30**

SD is the bright sunshine hours per day given as an input, DL is the maximum daylight hours, and R_a is the Extraterrestrial radiation. The calculations for DL and R_a are shown below:

Maximum Daylight Hours

$$DL = \frac{24}{\pi}\psi$$ **Equation 31**

where ψ is the sunset hour angle described by:

$$\psi = \arccos(-\tan\varphi \tan\delta)$$ **Equation 32**

φ is the latitude expressed in radians:

$$\varphi = \frac{L\pi}{180}$$ **Equation 33**

and δ is the solar declination angle:

$$\delta = 0.4093 \sin\left(\frac{2\pi}{365} J - 1.405\right)$$ **Equation 34**

Extraterrestrial radiation (MJ/m²d)

$$R_a = 37.586 d(\psi \sin\varphi \sin\delta + \cos\varphi \cos\delta \sin\psi)$$ **Equation 35**

where d is the relative distance between the earth and sun, calculated by:

$$d = 1 + 0.033 \cos\left(\frac{2\pi}{365} J\right)$$ **Equation 36**

Net outgoing long-wave radiation (MJ/m²d)

$$R_{ne} = 4.903 \cdot 10^{-9}\left(0.1 + 0.9\frac{SD}{DL}\right)(0.34 - 0.139\sqrt{e_d})\frac{(T_{kx})^4 + (T_{kn})^4}{2}$$ **Equation 37**

where:

$$T_{kx} = 273.16 + T_{\max}$$ **Equation 38**

$$T_{kn} = 273.16 + T_{\min}$$ **Equation 39**

Soil heat flux

$$G = 0.14(T_{a,n} - T_{a,n-1})$$ **Equation 40**

where $T_{a,n}$ and $T_{a,n-1}$ are average monthly temperatures of the current and previous months, respectively.

Once the potential evapotranspiration of a reference crop has been calculated, it is transformed into actual evapotranspiration by multiplying it with a soil moisture coefficient (k_s) and a crop coefficient (k_c):

$$Et = k_s k_c Et_0$$ **Equation 41**

The calculation of these coefficients is quite simple in CHARM. The crop coefficient is set to an annual constant value currently, and the soil moisture coefficient is calculated as pictured in Figure 18 (Martin, 1992):

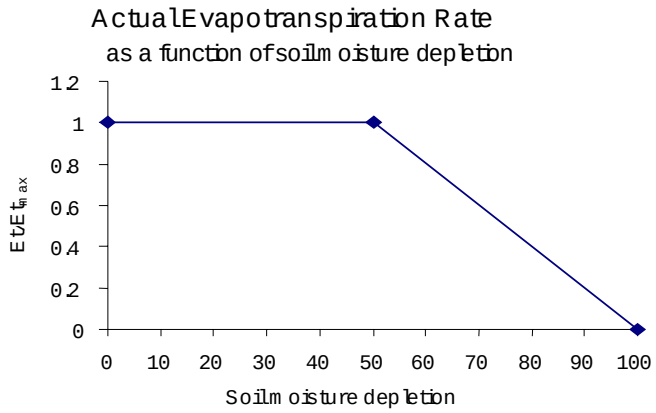

Figure 18: Actual evapotranspiration rate as a function of soil moisture depletion.

As the soil moisture is depleted, further evapotranspiration becomes increasingly difficult. Water is retained in the soil by capillary action, adhesion, and cohesion. As Figure 18 shows, in CHARM once the soil moisture is 50% depleted, evapotranspiration decreases linearly until there is no more water left in the soil to deplete. The soil moisture coefficient can be described mathematically by the following equation:

$$k_s = \begin{cases} 1 & if\ z > 0.5 \\ 2z & if\ z <= 0.5 \end{cases}$$ **Equation 42**

where, from equation 1, z is the relative soil storage, or $z = S/S_{max}$.